Electronic Supplementary Material (ESI) for Chemical Science.

Synthesis and Structural Characterization of Stable Coinage Metal (Cu, Ag, Au) Cyclopentadienyl Complexes

Robin Sievers, Marc Reimann, Nico G. Kub, Susanne M. Rupf, Martin Kaupp, Moritz Malischewski*

Contents

General Information 1
Synthetic Procedures 3
NMR Spectra 8
IR Spectra 21
Crystallographic Data 24
DFT Calculations 29
References 32

General Information

All Reactions and workups (except the recrystallization of $[NEt_4][C_5(CF_3)_5]$) were performed in previously heated glassware under an atmosphere of argon using standard Schlenk techniques and an oil pump vacuum of 10^{-3} mbar. Room temperature (rt) refers to 25 °C. The addition of liquid reagents and solvents was done by using threefold argon-flushed disposable syringes and septa, while solids were added in argon stream. Low temperature reactions were performed in a cooled ethanol-bath. Glassware was cleaned by storing in a potassium hydroxide bath for several days, rinsed with diluted hydrochloric acid and doubly deionized water and dried at 150 °C.

Pressure reactions

The synthesis of $[NEt_4][C_5(CF_3)_5]$ involves high temperatures and highly volatile substances in a closed system. Hence, it must be assumed, that high pressures arise upon heating and advanced caution is required. Therefore, it is advisable to perform the reaction in a separate and properly closed fumehood. The thick-walled glass reaction vessel should not be opened and if possible, not even touched until the reaction has finished and reached rt.

Solvents and reagents

Anhydrous MeCN, CH_2Cl_2 and *n*-pentane were obtained from the solvent system FMBRAUN MB SPS-800 and stored over activated 3 Å mol sieves. Anhydrous Et_2O was distilled under an atmosphere of argon over sodium using benzophenone as an indicator and stored over activated 3 Å mol sieves. Deuterated solvents CD_2Cl_2 and $CDCl_3$ were used as purchased and stored over activated 3 Å mol sieves. Solvents were degassed by three freeze-pump-thaw cycles. Sulfolane was heated at 60 °C for at least 24 h over activated 3 Å mol sieves and additionally 1 h in high vacuum prior to use. 18-crown-6 was heated at 80 °C for 2 h in high vacuum prior to use. All other solvents and commercially available reagents were used without further purification.

Nuclear magnetic resonance (NMR) spectroscopy

NMR spectroscopy was measured on a JEOL ECX 400 (400 MHz) or a Varian INOVA 600 (600 MHz) in the reported deuterated solvents $CDCl_3$ and CD_2Cl_2. All given chemical shifts in ^{1}H NMR spectra are calibrated on the resonance signals of $CHCl_3$ contained in $CDCl_3$ (δ = 7.26 ppm) and $CDHCl_2$ contained in CD_2Cl_2 (δ = 5.32 ppm). The ^{13}C NMR spectra are calibrated on the respective resonance signals of $CDCl_3$ (δ = 77.16 ppm), CD_2Cl_2 (δ = 53.84 ppm).[1,2] The ^{19}F and ^{31}P NMR spectra are device-internally calibrated relative to the resonance signal of $CFCl_3$ and H_3PO_4 according to the unified chemical shift scale.[3] The given multiplicities are phenomenological, thus the actual appearance of the signals is stated and not the theoretically expected one. The following abbreviations were used and analogously combined to designate multiplicities: s (singlet), d (doublet), t (triplet), q (quartet), m (multiplet), m_s (symmetric multiplet). For centrosymmetric multiplets the center and for non-symmetric multiplets the interval is stated. Evaluation of spectra was performed with Mestrelab Research MNova 7.[4]

Infrared (IR) spectroscopy

IR spectroscopy was measured on a FT (Fourier transformation) Nicolet iS10. The sample was directly measured by ATR (attenuated total reflection) technique. Characteristic absorptions are given in wavenumbers $\tilde{\nu}$ [cm^{-1}] and intensities are stated as vs (very strong), s (strong), m (medium) and w (weak).

High resolution mass spectroscopy (HRMS) and elemental analysis (EA)

HRMS was recorded using an AGILENT 6210 spectrometer by electrospray ionization (ESI) or an VARIAN MAT 711 by electron impact ionization (EI) at the department of mass spectroscopy at the Freie Universität Berlin. A detailed listing of fragmentation is dispensed, instead the molecular ion peak or a characteristic fragment peak is stated. EA was measured on a VARIO EL. Relative proportion of C and H are given in percent.

X-ray diffraction (XRD)

X-Ray data were collected on a BRUKER D8 Venture system. Data were collected at 105(2) K using graphite monochromated Mo K_α radiation (λ_α = 0.71073 Å). The strategy for the data collection was evaluated by using the Smart software. The data were collected by the standard "*ψ-ω* scan techniques" and were scaled and reduced using Saint+software. The structures were solved by using Olex2,[5] the structure was solved with the XT[6] structure solution program using Intrinsic Phasing and refined with the XL refinement package[7,8] using Least Squares minimization. Bond length and angles were measured with Diamond Crystal and Molecular Structure Visualization Version 4.6.2.[9] Drawings were generated with POV-Ray.[10]

Density functional theory (DFT) calculations

Structure optimizations were performed at the r^{2}SCAN-3c[11] composite DFT level using the ADF engine of the AMS program package.[12,13] For this purpose, Gasevic *et al.* have prescribed tailor-made mTZ2P Slater-type basis sets, D4 dispersion corrections, and a geometrical counterpoise (gCP) correction.[11] The SCF was converged to a DIIS error below 10^{-7} and the structure optimizations used "good" convergence criteria. The numerical quality was set to "good". Scalar relativistic effects were included using the ZORA Hamiltonian unless explicitly stated otherwise.[14] All structures were characterized as minima by performing harmonic vibrational frequency calculations using numerical second derivatives of analytical gradients. Natural population analyses (NPA)[15] were performed at the same level using the optimized structures. Energy decomposition analyses (EDA)[16] were performed using the two closed-shell, singly charged units of $[M\text{-}PMe_3]^+$ (M = Cu, Ag, Au) and $[C_5(CX_3)_5]^-$ (X = H, F). Additional single point calculations were performed using the PNO-CCSD(T*)-F12b approach[17,18] and the MOLPRO program package, release 2022.2.[19,20] These calculations employed cc-pVTZ-F12 GTO basis sets[21] as well as the auxiliary basis sets assigned by the program.

Synthetic Procedures

Tetraethylammonium 1,2,3,4,5-pentakis(trifluoromethyl)cyclopentadienide

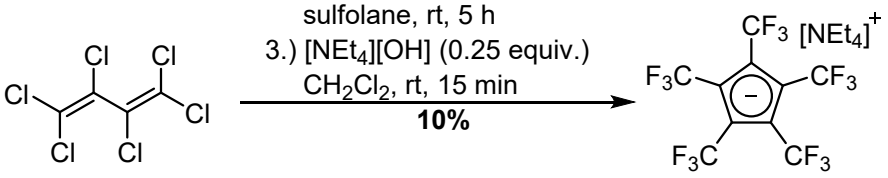

In a dried 1000 mL pressure flask anhydrous KF (60 g, 1.0 mol, 11 equiv.) was placed in anhydrous and degassed sulfolane (190 mL) under an atmosphere of argon. Anhydrous and degassed 18-crown-6 (8.7 g, 33 mmol, 0.33 equiv.) and hexachlorobuta-1,3-diene (15 mL, 96 mmol, 1.0 equiv.) were added at rt. The resulting reaction mixture was carefully shaken and cooled to −196 °C in high vacuum. The properly closed pressure flask was slowly warmed to 190 °C and stirred at this temperature for 4 d. Then the resulting black suspension was cooled to rt and the volatiles were removed in high vacuum. The remaining mixture was filtrated under an atmosphere of argon and the residue was extracted with anhydrous MeCN (3 × 40 mL). The filtrate was warmed to 40 °C and all MeCN was removed in high vacuum, while stirring. The resulting solution was put under high vacuum and H_2SO_4 (conc., 200 mL, 3.6 mol, 38 equiv.) was added dropwise at rt over a period of 3 h, while stirring and continuously collecting the volatiles in a cold trap of −196 °C. After complete addition, the mixture remained for additional 2 h in high vacuum. The cold trap was put under argon and slowly warmed to 0 °C, giving a pale yellow liquid. Then CH_2Cl_2 (20 mL) and a solution of $[NEt_4][OH]$ (35% in water, 10 mL, 24 mmol, 0.25 equiv.) were added and the reaction mixture was stirred for 15 min at rt, giving a deep red solution. The aqueous layer was separated and extracted with CH_2Cl_2 (4 × 20 mL). The combined organic layers were dried over $MgSO_4$, filtrated and the solvent was removed under reduced pressure. The remaining solid was suspended in Et_2O (~5 mL) and recrystallized twice from CH_2Cl_2 (~10 mL) by slowly cooling to −20 °C. The crystalline residue was decanted and washed with Et_2O (2 × 5 mL). The solvents were removed under reduced pressure to give product $[NEt_4][C_5(CF_3)_5]$ (2.0 g, 3.7 mmol) as a colorless crystalline solid with a yield of 10%.[22]

^{1}H NMR (400 MHz, CD_2Cl_2, rt) δ [ppm] = 2.95 (q, $^3J_{H,H}$ = 7.3 Hz, 8H, Et (CH_2)), 1.19 (q, $^3J_{H,H}$ = 7.1 Hz, 12H, Et (CH_3)). **^{13}C{^{1}H} NMR** (151 MHz, CD_2Cl_2, rt) δ [ppm] = 52.7 (m_s, Et (CH_2)), 7.3 (s, Et (CH_3)). **^{13}C{^{19}F} NMR** (151 MHz, CD_2Cl_2, rt) δ [ppm] = 124.9 (s, Cp (CF_3)), 109.6 (s, Cp (C_5)). **^{19}F NMR** (377 MHz, CD_2Cl_2, rt) δ [ppm] = −50.6 (s).

The analytical data are consistent with those reported in literature.[23–25]

Acetato-tris(*tert*-butyl)phosphine-copper(I)

$$[CuOAc] \xrightarrow[Et_2O,\ -20\ °C \rightarrow rt,\ 3\ h]{P^tBu_3\ (1.0\ equiv.)} [Cu(P^tBu_3)(OAc)]$$

72%

In a dried 10 mL Schlenk flask [CuOAc] (50 mg, 0.41 mmol, 1.0 equiv.) was suspended in anhydrous and degassed Et_2O (3 mL) under an argon atmosphere and cooled to −20 °C. Then P^tBu_3 (83 mg, 0.41 mmol, 1.0 equiv.) was added and the reaction mixture was stirred at this temperature for 3 h. The resulting greenish suspension was filtrated under an argon atmosphere and the solvent of the filtrate was removed in high vacuum. The remaining solid was washed with anhydrous *n*-pentane (5 × 2 mL) and the solvent was removed in high vacuum to give product [Cu(P^tBu_3)(OAc)] (97 mg, 0.30 mmol) as a colorless solid with a yield of 72%.

^{1}H NMR (400 MHz, $CDCl_3$, rt) δ [ppm] = 2.05 (s, 3H, OAc), 1.47 (d, $^3J_{H,P}$ = 13.0 Hz, 27H, ^{t}Bu). **^{13}C{^{1}H} NMR** (176 MHz, $CDCl_3$, rt) δ [ppm] = 37.3 (d, $^1J_{C,P}$ = 13.4 Hz, ^{t}Bu (C)), 32.4 (d, $^2J_{C,P}$ = 5.6 Hz, ^{t}Bu (CH_3)), 29.3 (s, OAc (CH_3)).[26] **^{31}P{^{1}H} NMR** (162 MHz, $CDCl_3$, rt) δ [ppm] = 73.0 (s). **FT-IR** (ATR) $\tilde{\nu}$ [cm^{-1}] = 575 (m), 601 (m), 650 (m), 806 (m), 927 (w), 1022 (w), 1171 (m), 1309 (w), 1336 (w), 1366 (m), 1406 (vs), 1483 (m), 1592 (vs), 2869 (w), 2901 (w), 2953 (w), 2991 (w). **HRMS** (ESI-TOF, positive) m/z for $[C_{12}H_{27}PCu]^+$ calculated: 265.1146; measured: 265.1386. **EA** [$C_{14}H_{30}PCu$] calculated: C: 51.75%, H: 9.31%; measured: C: 51.77%, H: 10.59%.

Acetato-tris(*tert*-butyl)phosphine-silver(I)

$$[AgOAc] \xrightarrow[CH_2Cl_2,\ rt,\ 18\ h]{P^tBu_3\ (1.0\ equiv.)} [Ag(P^tBu_3)(OAc)]$$

quant.

In a dried 10 mL Schlenk flask [AgOAc] (68 mg, 0.41 mmol, 1.0 equiv.) and P^tBu_3 (83 mg, 0.41 mmol, 1.0 equiv.) were placed in anhydrous and degassed CH_2Cl_2 (2 mL) under an argon atmosphere. Then the reaction mixture was stirred at room temperature under exclusion of light for 18 h. The resulting colorless solution was filtrated under an argon atmosphere and the solvent of the filtrate was removed in high vacuum. The remaining solid was washed with anhydrous *n*-pentane (5 × 2 mL) and the solvent was removed in high vacuum to give product [Ag(P^tBu_3)(OAc)] (0.15 g, 0.41 mmol) as a colorless solid with a quantitative yield.

^{1}H NMR (400 MHz, $CDCl_3$, rt) δ [ppm] = 2.07 (s, 3H, OAc), 1.47 (d, $^3J_{H,P}$ = 13.5 Hz, 27H, ^{t}Bu). **^{13}C{^{1}H} NMR** (101 MHz, $CDCl_3$, rt) δ [ppm] = 180.3 (s, OAc (CO_2)), 37.5 (dd, $^1J_{C,P}$ = 7.3 Hz, $^2J_{C,Ag}$ = 4.4 Hz, ^{t}Bu (C)), 32.4 (dd, $^2J_{C,P}$ = 7.1 Hz, $^3J_{C,Ag}$ = 2.4 Hz, ^{t}Bu (CH_3)), 29.3 (s, OAc (CH_3)). **^{31}P{^{1}H} NMR** (162 MHz, $CDCl_3$, rt) δ [ppm] = 85.1 (d, $^1J_{P,^{107}Ag}$ = 644.0 Hz, $^1J_{P,^{109}Ag}$ = 743.4 Hz).

The analytical data are consistent with those reported in literature.[27]

Acetato-tris(*tert*-butyl)phosphine-gold(I)

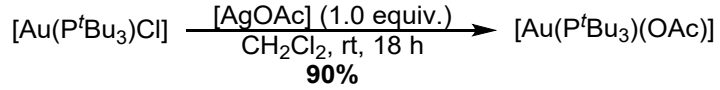

In a dried 10 mL Schlenk flask [Au(P^{t}Bu$_3$)Cl] (100 mg, 0.23 mmol, 1.0 equiv.) and [AgOAc] (38 mg, 0.23 mmol, 1.0 equiv.) were placed in anhydrous and degassed CH_2Cl_2 (2 mL) under an argon atmosphere. Then the reaction mixture was stirred at room temperature under exclusion of light for 18 h. The resulting colorless suspension was filtrated under an argon atmosphere and the solvent of the filtrate was removed in high vacuum. The remaining solid was washed with anhydrous *n*-pentane (5 × 2 mL) and the solvent was removed in high vacuum to give product [Au(P^{t}Bu$_3$)(OAc)] (96 mg, 0.21 mmol) as a colorless solid with a yield of 90%.

^{1}H NMR (400 MHz, $CDCl_3$, rt) δ [ppm] = 2.03 (s, 3H, OAc), 1.47 (d, $^3J_{H,P}$ = 13.8 Hz, 27H, ^{t}Bu). **^{13}C{^{1}H} NMR** (101 MHz, $CDCl_3$, rt) δ [ppm] = 177.2 (d, $^3J_{C,P}$ = 3.3 Hz, OAc (CO_2)), 39.5 (d, $^1J_{C,P}$ = 22.3 Hz, ^{t}Bu (C)), 32.3 (d, $^2J_{C,P}$ = 3.6 Hz, ^{t}Bu (CH_3)), 24.2 (d, $^4J_{C,P}$ = 5.2 Hz, OAc (CH_3)). **^{31}P{^{1}H} NMR** (162 MHz, $CDCl_3$, rt) δ [ppm] = 85.4 (s). **FT-IR** (ATR) $\tilde{\nu}$ [cm^{-1}] = 530 (m), 592 (m), 678 (s), 809 (m), 933 (w), 1029 (w), 1174 (m), 1309 (vs), 1369 (s), 1393 (m), 1444 (w), 1482 (w), 1628 (vs), 2874 (w), 2923 (w), 2968 (w), 2996 (w). **HRMS** (EI-TOF, positive) m/z for $[C_{12}H_{27}PAu]^+$ calculated: 399.1516; measured: 399.1451. **EA** [$C_{14}H_{30}PAu$] calculated: C: 36.69%, H: 6.60%; measured: C: 36.83%, H: 6.43%.

η^3/η^2-Pentakis(trifluoromethyl)cyclopentadienyl-tris(*tert*-butyl)phosphine-copper(I)

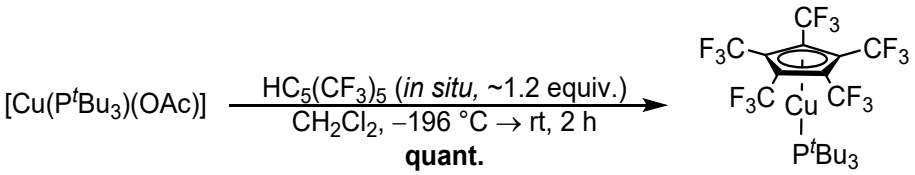

In a dried 10 mL Schlenk flask H_2SO_4 (conc., 2.0 mL, exc.) was placed under an argon atmosphere and cooled to −196 °C before [NEt_4][$C_5(CF_3)_5$] (100 mg, 0.19 mmol, 1.4 equiv.) was added. Then the reaction mixture was warmed to rt under high vacuum and stirred at this temperature for 20 min. The volatiles where continuously trapped in a second dried 10 mL Schlenk flask cooled to −196 °C, containing [Cu(P^{t}Bu$_3$)(OAc)] (43 mg, 0.13 mmol, 1.0 equiv.) in anhydrous and degassed CH_2Cl_2 (2 mL). The second Schlenk flask was put under an atmosphere of argon, warmed to rt and stirred at this temperature for 2 h under the exclusion of light. The solvent was removed in high vacuum and the remaining solid was washed with anhydrous and degassed *n*-pentane (3 × 2 mL). The solvent was removed in high vacuum to give product [Cu($C_5(CF_3)_5$)(P^{t}Bu$_3$)] (87 mg, 0.13 mmol) as a colorless solid with a quantitative yield.[28]

^{1}H NMR (400 MHz, CD_2Cl_2, rt) δ [ppm] = 1.34 (d, $^3J_{H,P}$ = 13.7 Hz, ^{t}Bu). **^{13}C{^{1}H} NMR** (176 MHz, CD_2Cl_2, rt) δ [ppm] = 122.1 (q, $^1J_{C,F}$ = 275.5 Hz, Cp (CF_3)), 110.3–109.1 (m, Cp (C_5)), 37.5 (d, $^1J_{C,P}$ = 13.7 Hz, ^{t}Bu (C)), 32.4 (d, $^2J_{C,P}$ = 4.4 Hz, ^{t}Bu (CH_3)). **^{19}F NMR** (377 MHz, CD_2Cl_2, rt) δ [ppm] = –50.9 (s). **^{31}P{^{1}H} NMR** (162 MHz, CD_2Cl_2, rt) δ [ppm] = 79.5 (s). **FT-IR** (ATR) $\tilde{\nu}$ [cm^{-1}] = 633 (w), 806 (m), 938 (w), 951 (m), 1020 (m), 1138 (vs), 1207 (vs), 1375 (m), 1401 (m), 1450 (w), 1482 (m), 2880 (w), 2912 (w), 2966 (w), 3006 (w). **HRMS** (ESI-TOF, positive) m/z for $[C_{12}H_{27}PCu]^+$ calculated: 265.1146; measured: 265.1107. **HRMS** (ESI-TOF, negative) m/z for $[C_{10}F_{15}]^-$ calculated: 404.9760; measured: 404.9251. **EA** $[C_{22}H_{27}F_{15}PCu]$ calculated: C: 39.38%, H: 4.06%; measured: C: 39.55%, H: 4.09%.

η^3/η^1-Pentakis(trifluoromethyl)cyclopentadienyl-tris(*tert*-butyl)phosphine-silver(I)

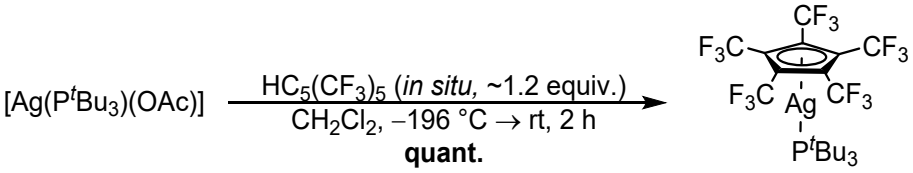

In a dried 10 mL Schlenk flask H_2SO_4 (conc., 2.0 mL, exc.) was placed under an argon atmosphere and cooled to −196 °C before $[NEt_4][C_5(CF_3)_5]$ (100 mg, 0.19 mmol, 1.4 equiv.) was added. Then the reaction mixture was warmed to rt under high vacuum and stirred at this temperature for 20 min. The volatiles where continuously trapped in a second dried 10 mL Schlenk flask cooled to −196 °C, containing $[Ag(P^tBu_3)(OAc)]$ (48 mg, 0.13 mmol, 1.0 equiv.) in anhydrous and degassed CH_2Cl_2 (2 mL). The second Schlenk flask was put under an atmosphere of argon, warmed to rt and stirred at this temperature for 2 h under the exclusion of light. The solvent was removed in high vacuum and the remaining solid was washed with anhydrous and degassed *n*-pentane (3 × 2 mL). The solvent was removed in high vacuum to give product $[Ag(C_5(CF_3)_5)(P^tBu_3)]$ (93 mg, 0.13 mmol) as a colorless solid with a quantitative yield.[28]

^{1}H NMR (400 MHz, CD_2Cl_2, rt) δ [ppm] = 1.34 (d, $^3J_{H,P}$ = 14.2 Hz, ^{t}Bu). **^{13}C{^{1}H} NMR** (151 MHz, CD_2Cl_2, rt) δ [ppm] = 122.4 (q, $^1J_{C,F}$ = 272.0 Hz, Cp (CF_3)), 112.0–110.8 (m, Cp (C_5)), 37.8 (dd, $^1J_{C,P}$ = 13.3 Hz, $^2J_{C,Ag}$ = 4.4 Hz, ^{t}Bu (C)), 32.3 (dd, $^2J_{C,P}$ = 8.8 Hz, $^3J_{C,Ag}$ = 3.6 Hz, ^{t}Bu (CH_3). **^{19}F NMR** (377 MHz, CD_2Cl_2, rt) δ [ppm] = –53.1 (s). **^{31}P{^{1}H} NMR** (162 MHz, CD_2Cl_2, rt) δ [ppm] = 92.8 (d, $^1J_{C,^{107}Ag}$ = 651.6 Hz, $^1J_{C,^{109}Ag}$ = 752.2 Hz). **FT-IR** (ATR) $\tilde{\nu}$ [cm^{-1}] = 632 (w), 718 (w), 731 (w), 747 (w), 803 (m), 937 (w), 1023 (m), 1149 (vs), 1205 (vs) 1288 (m), 1374 (m), 1397 (m), 1414 (w), 1483 (m), 1532 (w), 2883 (w), 2913 (w), 2961 (w), 3007 (w). **HRMS** (ESI-TOF, positive) m/z for $[C_{12}H_{27}PAg]^+$ calculated: 309.0901; measured: 309.2021. **HRMS** (ESI-TOF, negative) m/z for $[C_{10}F_{15}]^-$ calculated: 404.9760; measured: 404.9142. **EA** $[C_{22}H_{27}F_{15}PAg]$ calculated: C: 36.94%, H: 3.80%; measured: C: 36.96%, H: 3.86%.

***η*¹-Pentakis(trifluoromethyl)cyclopentadienyl-tris(*tert*-butyl)phosphine-gold(I)**

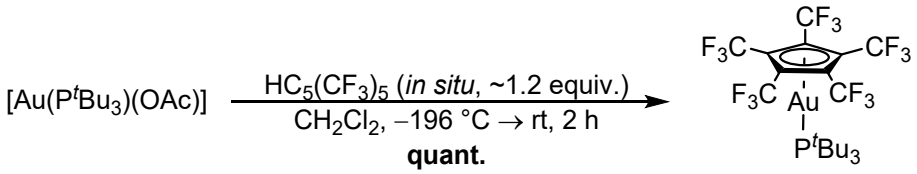

In a dried 10 mL Schlenk flask H_2SO_4 (conc., 2.0 mL, exc.) was placed under an argon atmosphere and cooled to −196 °C before $[NEt_4][C_5(CF_3)_5]$ (100 mg, 0.19 mmol, 1.4 equiv.) was added. Then the reaction mixture was warmed to rt under high vacuum and stirred at this temperature for 20 min. The volatiles where continuously trapped in a second dried 10 mL Schlenk flask cooled to −196 °C, containing $[Au(P^tBu_3)(OAc)]$ (60 mg, 0.13 mmol, 1.0 equiv.) in anhydrous and degassed CH_2Cl_2 (2 mL). The second Schlenk flask was put under an atmosphere of argon, warmed to rt and stirred at this temperature for 2 h under the exclusion of light. The solvent was removed in high vacuum and the remaining solid was washed with anhydrous and degassed *n*-pentane (3 × 2 mL). The solvent was removed in high vacuum to give product $[Au(C_5(CF_3)_5)(P^tBu_3)]$ (0.10 mg, 0.13 mmol) as a colorless solid with a quantitative yield.[28]

^{1}H NMR (400 MHz, CD_2Cl_2, rt) δ [ppm] = 1.41 (d, $^3J_{H,P}$ = 14.4 Hz, ^{t}Bu). **^{13}C{^{1}H} NMR** (176 MHz, CD_2Cl_2, rt) δ [ppm] = 121.7 (q, $^1J_{C,F}$ = 275.3 Hz, Cp (CF_3)), 115.8–114.5 (m, Cp (C_5)), 40.0 (d, $^1J_{C,P}$ = 19.1 Hz, ^{t}Bu (C)), 32.3 (d, $^2J_{C,P}$ = 3.6 Hz, ^{t}Bu (CH_3)). **^{19}F NMR** (377 MHz, CD_2Cl_2, rt) δ [ppm] = –51.9 (s). **^{31}P{^{1}H} NMR** (162 MHz, CD_2Cl_2, rt) δ [ppm] = 96.6 (s). **FT-IR** (ATR) $\tilde{\nu}$ [cm^{-1}] = 632 (w), 718 (w), 731 (w), 747 (w), 803 (m), 937 (w), 1023 (m), 1149 (vs), 1205 (vs), 1277 (m), 1374 (m), 1397 (m), 1414 (w), 1483 (m), 1532 (w), 2883 (w), 2913 (w), 2961 (w), 3007 (w). **HRMS** (ESI-TOF, positive) m/z for $[C_{12}H_{27}PAu]^+$ calculated: 399.2960; measured: 399.1484. **HRMS** (ESI-TOF, negative) m/z for $[C_{10}F_{15}]^-$ calculated: 404.9760; measured: 404.9137. **EA** $[C_{22}H_{27}F_{15}PAu]$ calculated: C: 32.85%, H: 3.38%; measured: C: 32.95%, H: 3.54%.

NMR Spectra

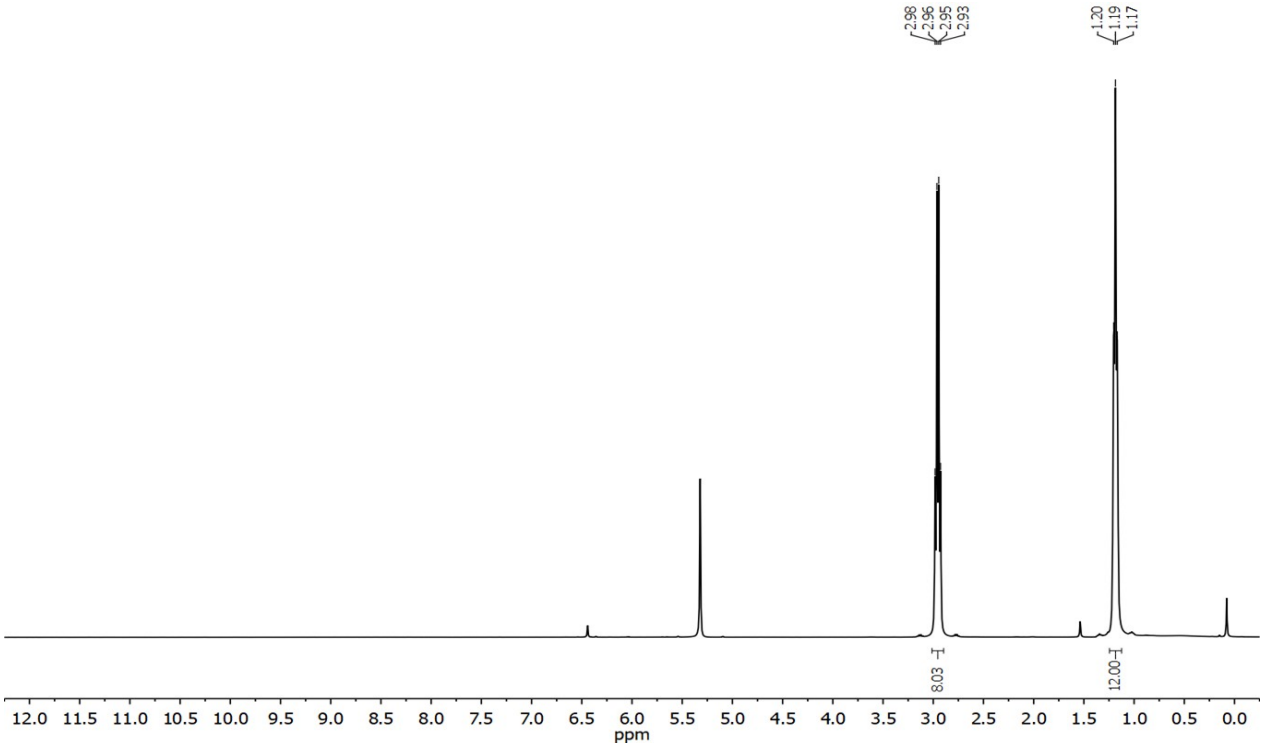

Figure S1. ^{1}H NMR (400 MHz, CD_2Cl_2, rt) spectrum of $[NEt_4][C_5(CF_3)_5]$.

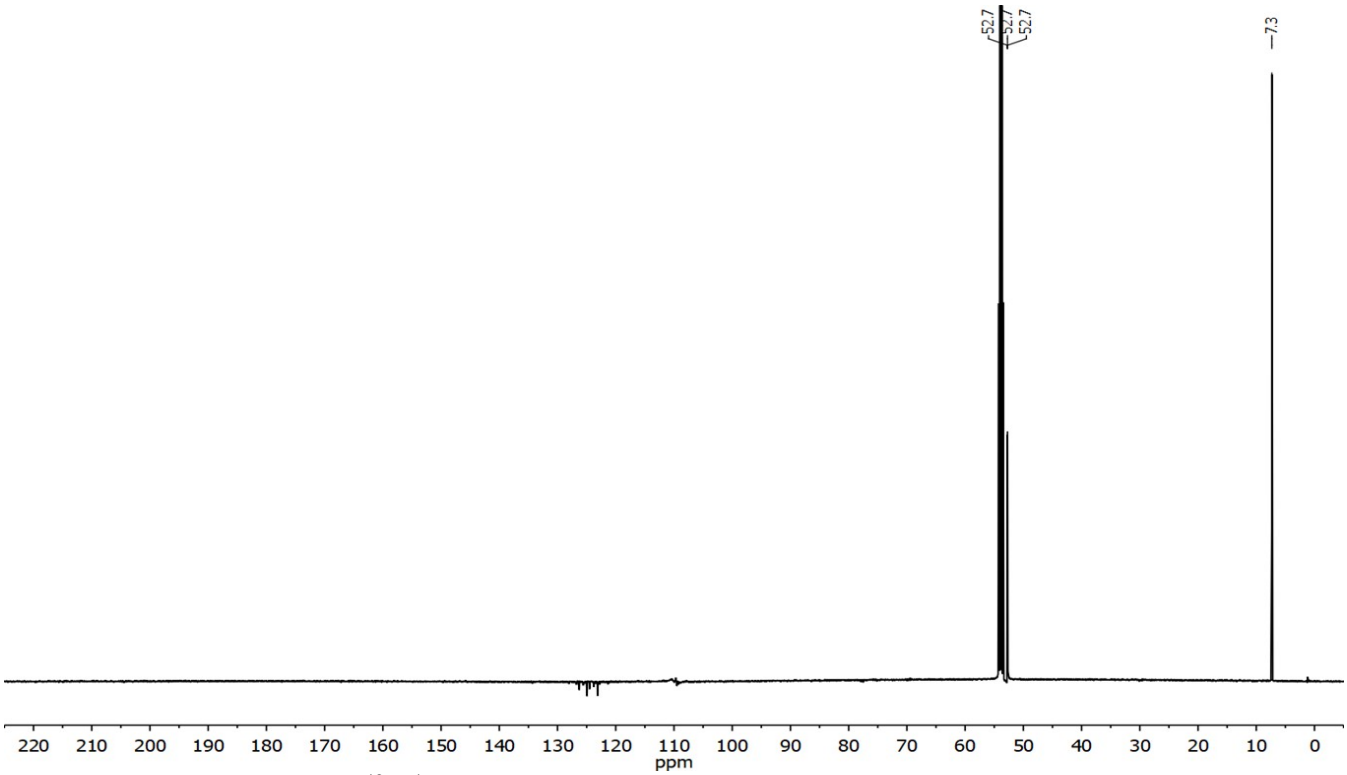

Figure S2. $^{13}C\{^{1}H\}$ NMR (151 MHz CD_2Cl_2, rt) spectrum of $[NEt_4][C_5(CF_3)_5]$.

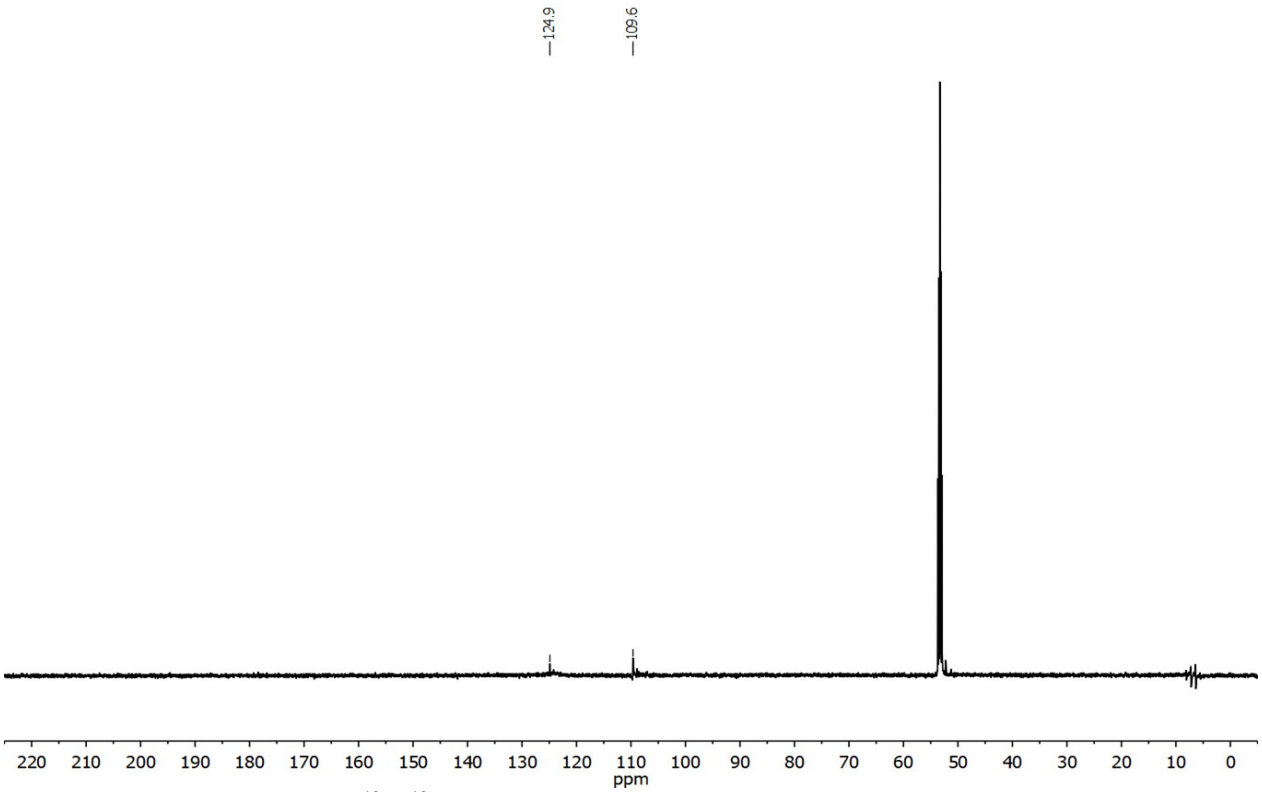

Figure S3. $^{13}C\{^{19}F\}$ NMR (151 MHz CD_2Cl_2, rt) spectrum of $[NEt_4][C_5(CF_3)_5]$.

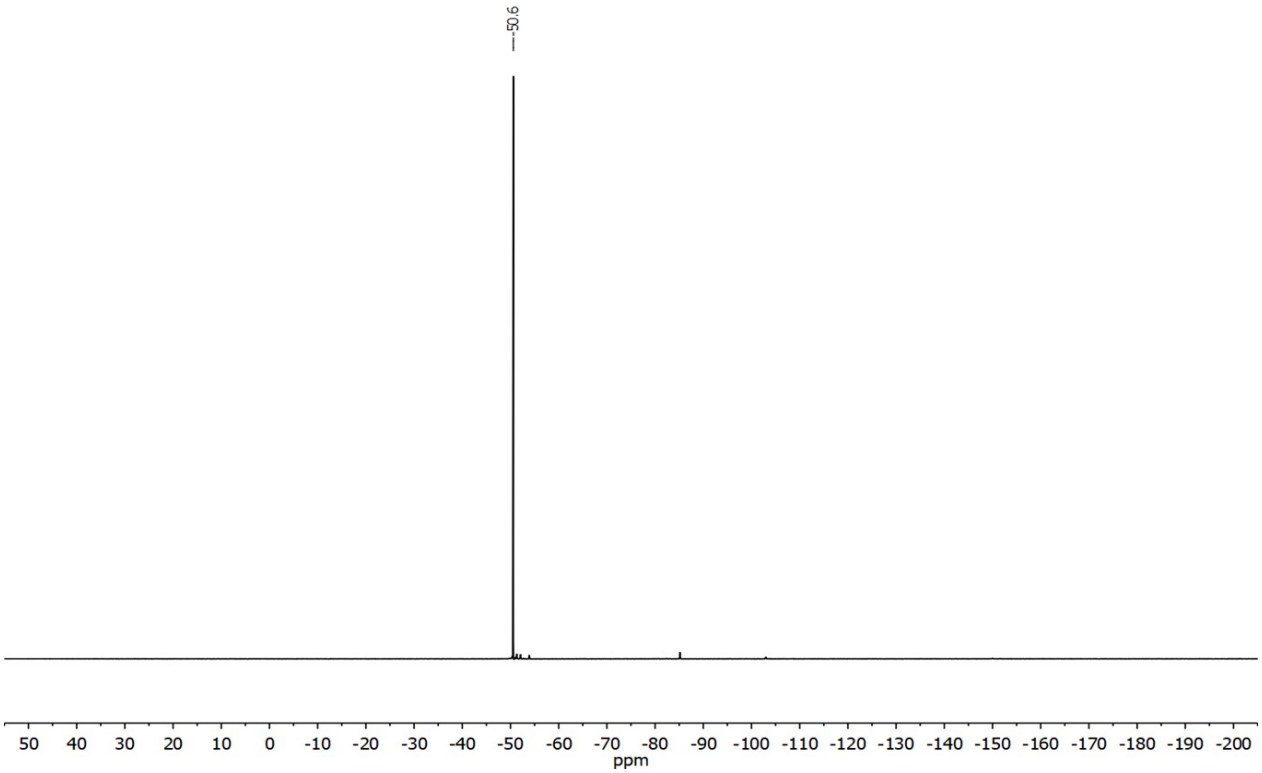

Figure S4. ^{19}F NMR (377 MHz, CD_2Cl_2, rt) spectrum of $[NEt_4][C_5(CF_3)_5]$.

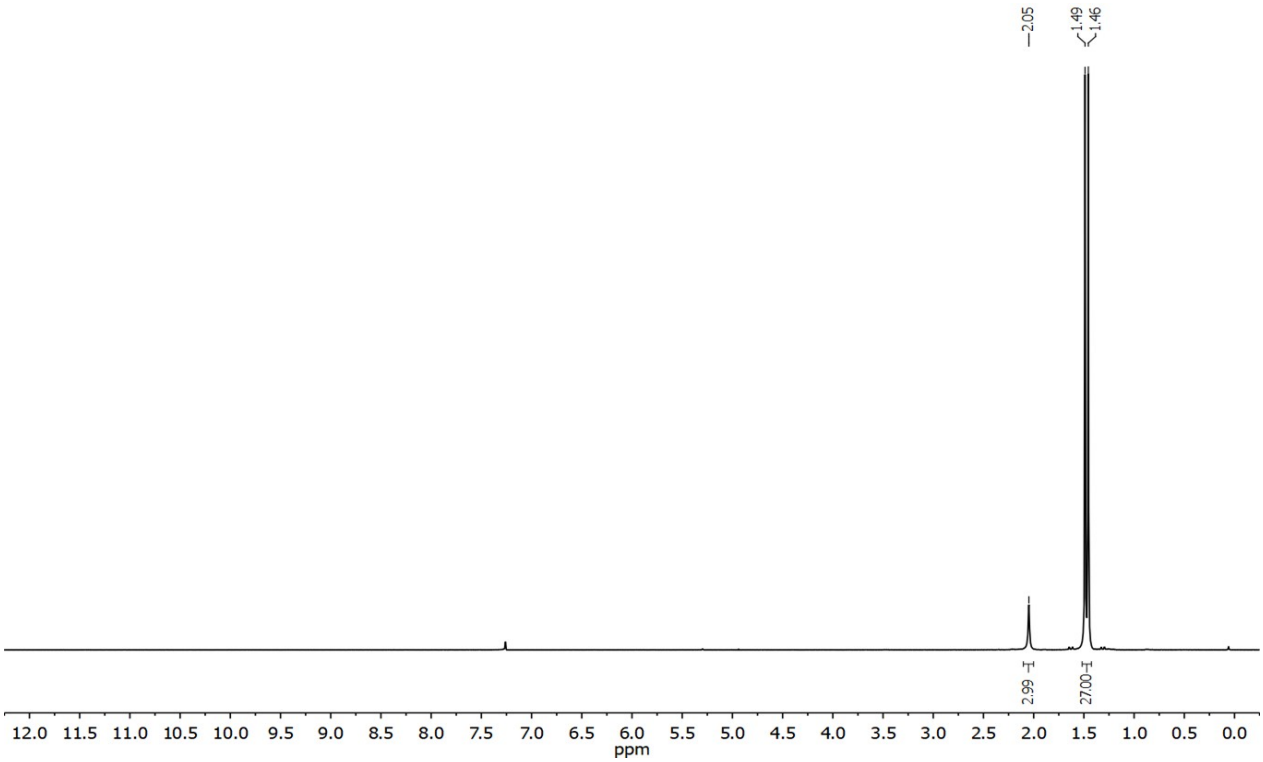

Figure S5. ^{1}H NMR (400 MHz, $CDCl_3$, rt) spectrum of [Cu(P^tBu_3)(OAc)].

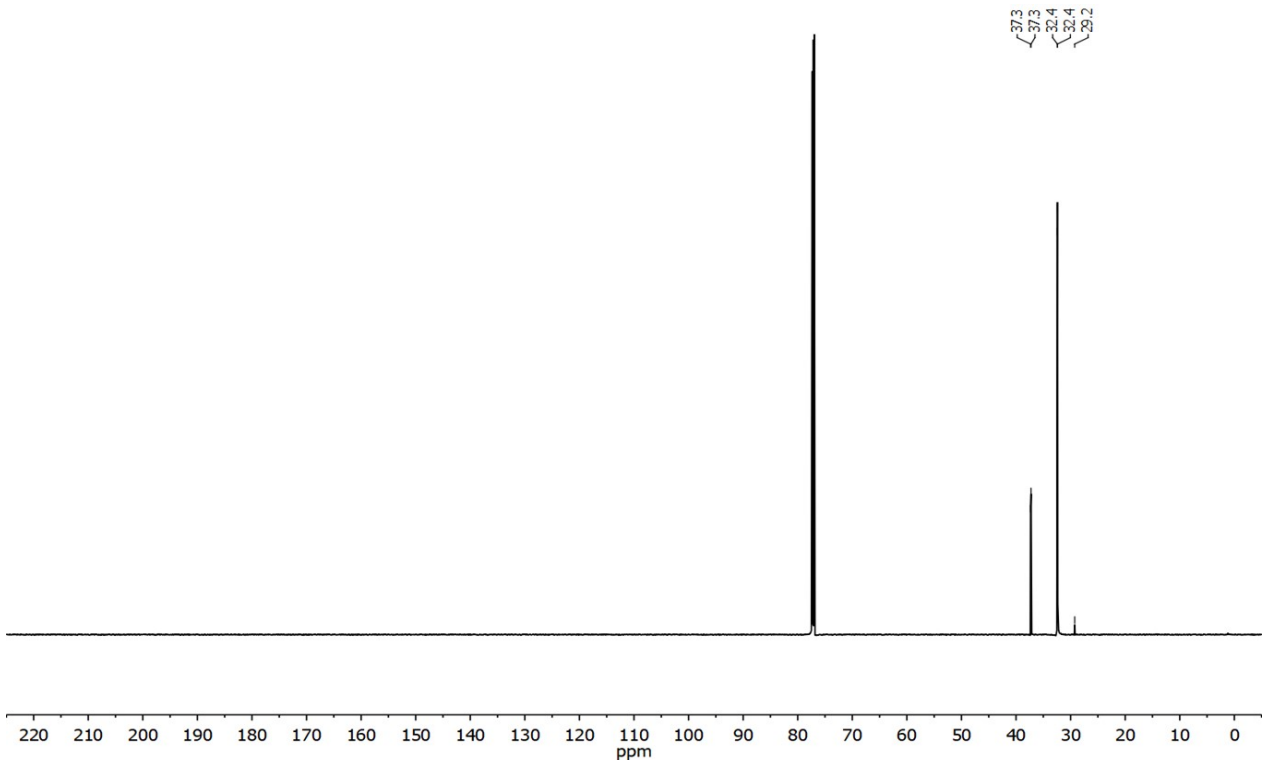

Figure S6. $^{13}C\{^{1}H\}$ NMR (176 MHz, $CDCl_3$, rt) spectrum of [Cu(P^tBu_3)(OAc)].

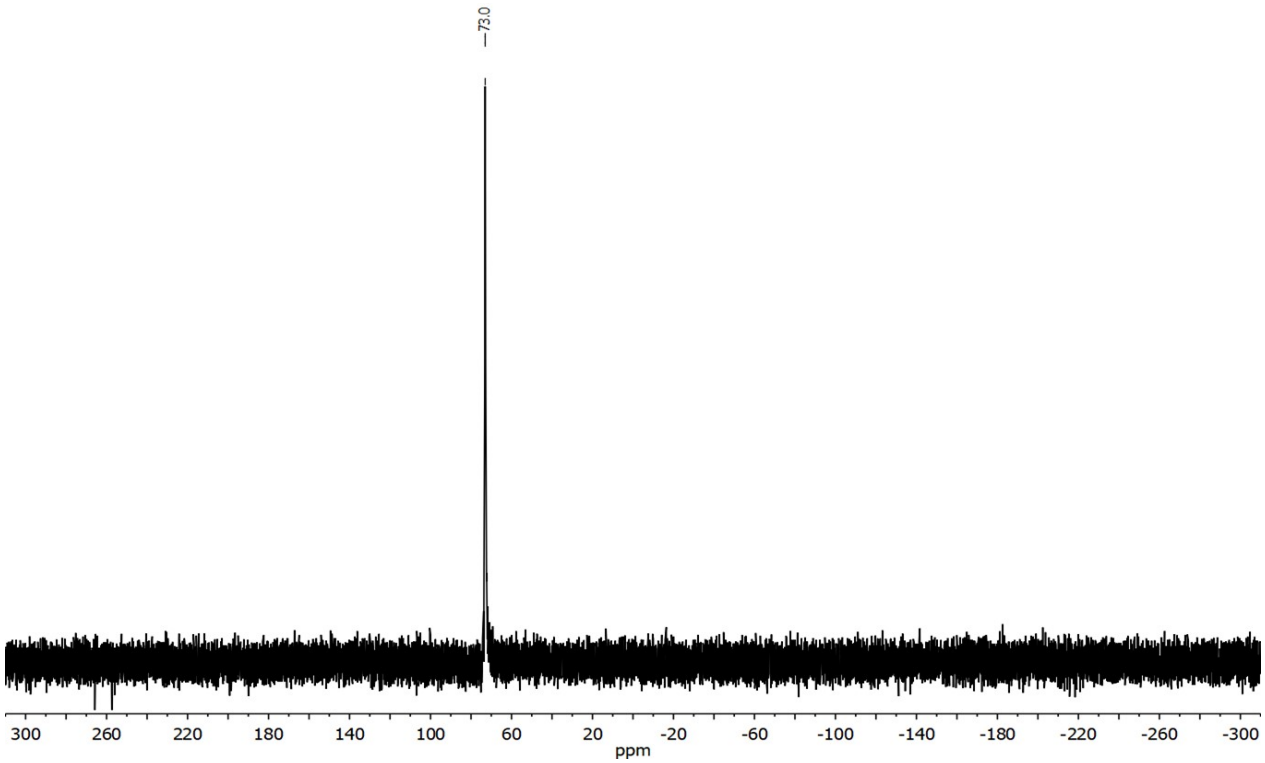

Figure S7. $^{31}P\{^{1}H\}$ NMR (162 MHz, $CDCl_3$, rt) spectrum of [Cu(P^tBu_3)(OAc)].

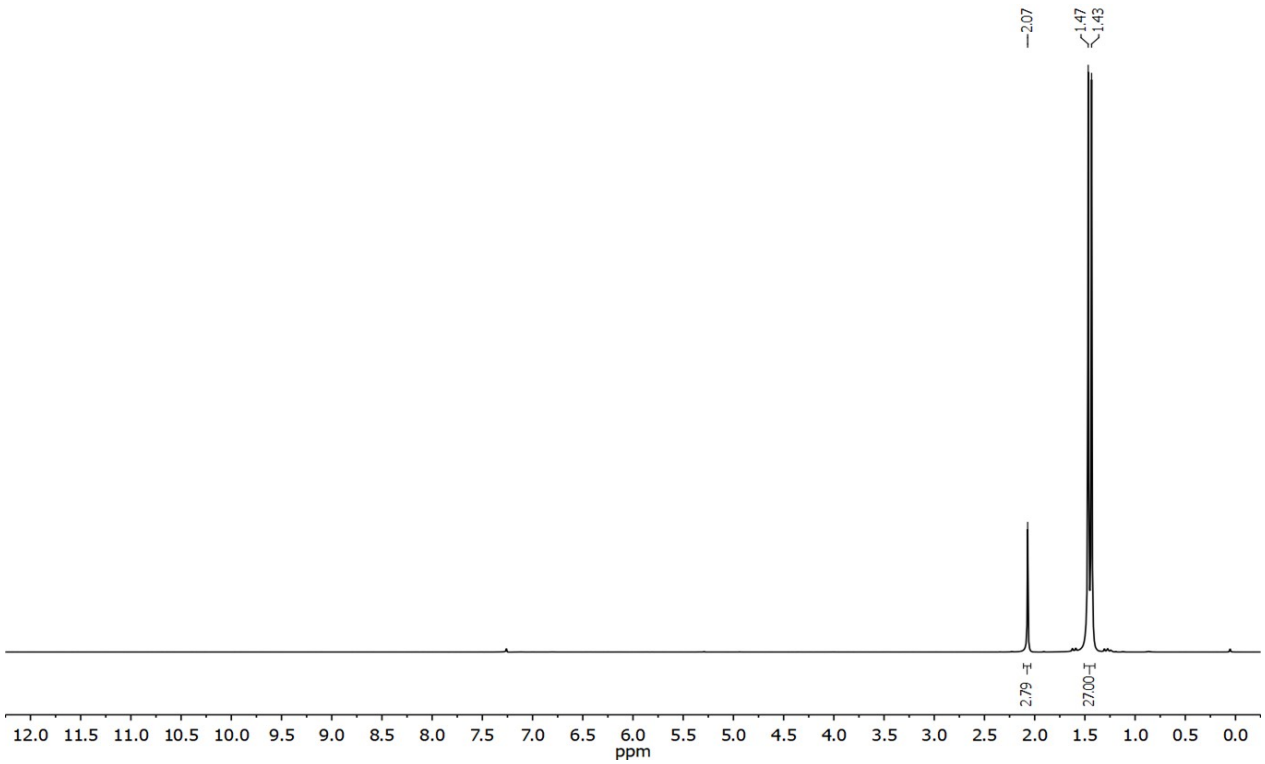

Figure S8. ^{1}H NMR (400 MHz, $CDCl_3$, rt) spectrum of [Ag(P^tBu_3)(OAc)].

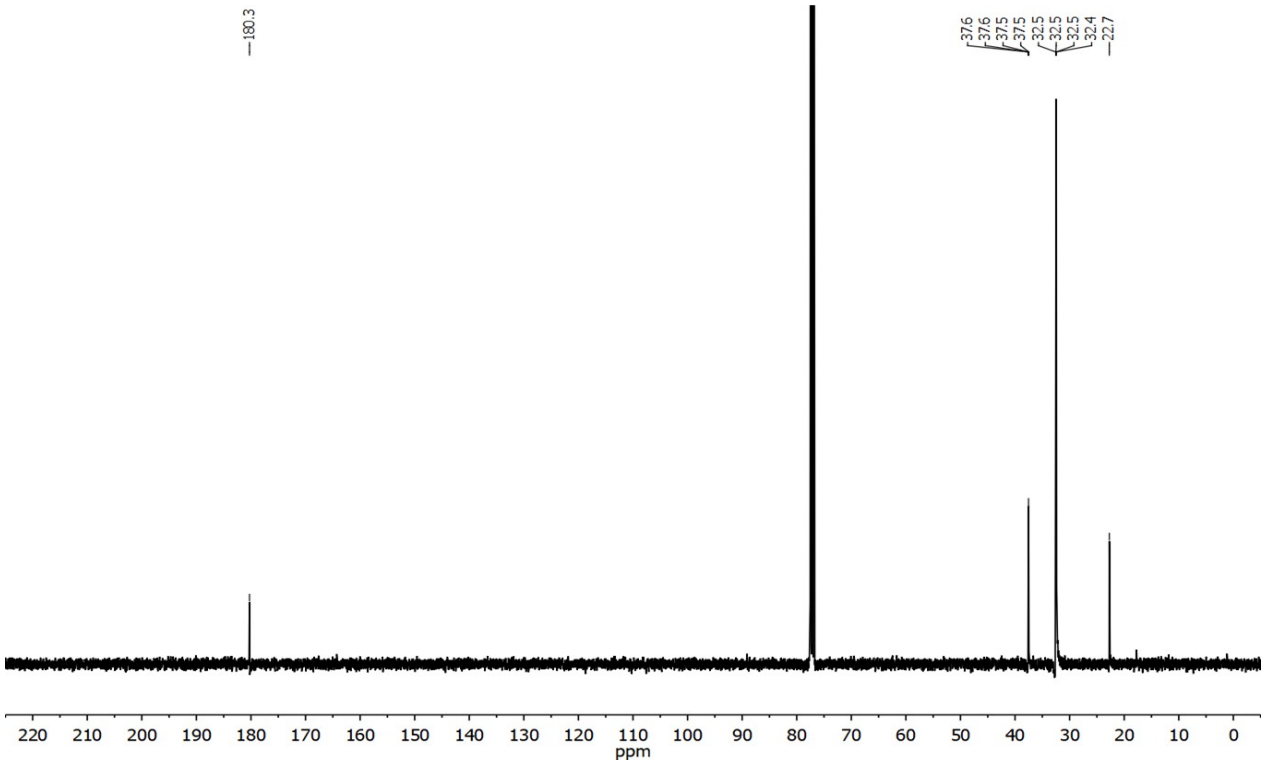

Figure S9. $^{13}C\{^{1}H\}$ NMR (101 MHz, $CDCl_3$, rt) spectrum of [Ag(P^tBu_3)(OAc)].

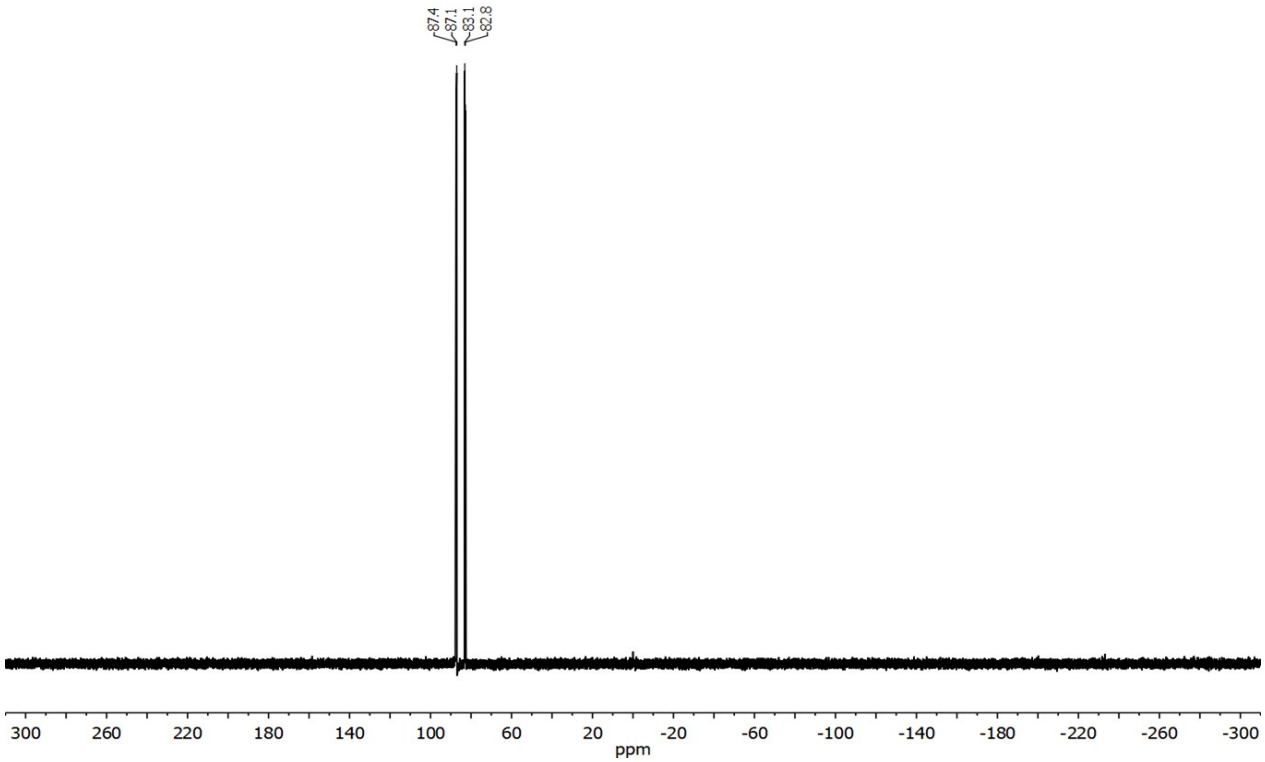

Figure S10. $^{31}P\{^{1}H\}$ NMR (162 MHz, $CDCl_3$, rt) spectrum of [Ag(P^tBu_3)(OAc)].

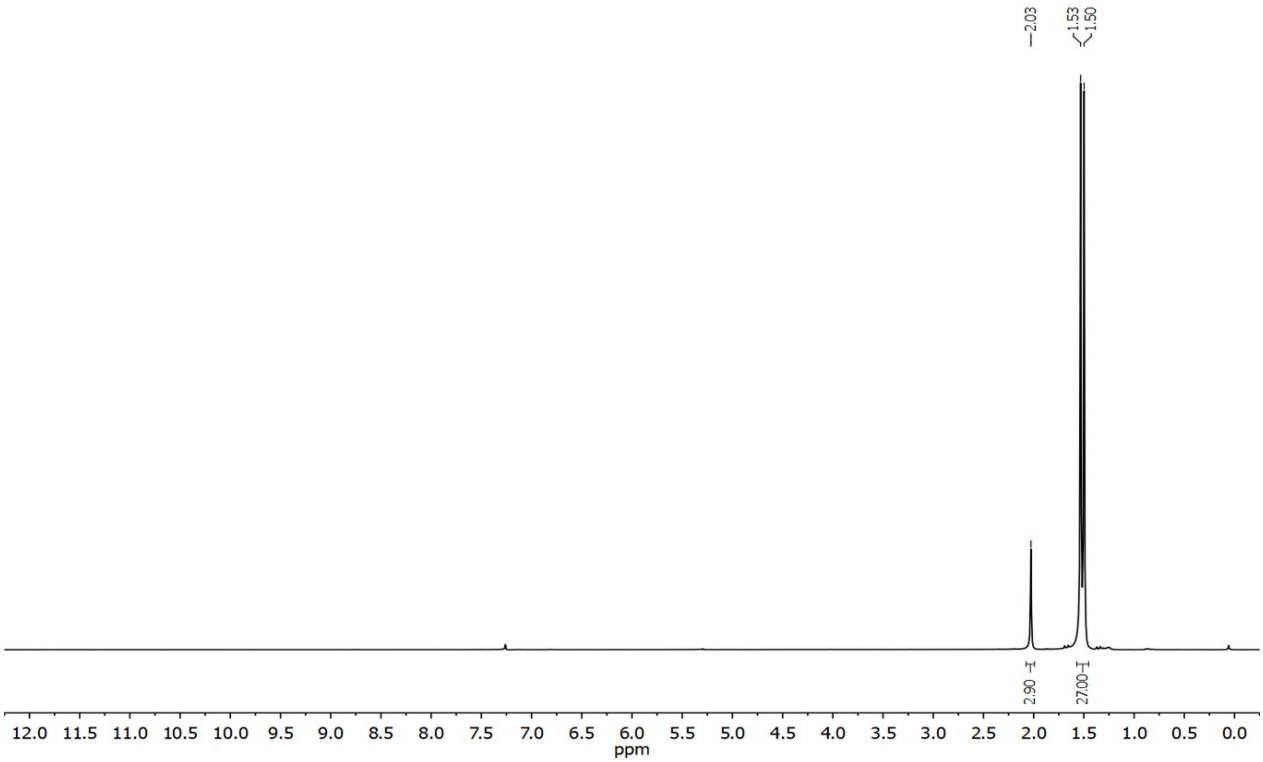

Figure S11. ^{1}H NMR (400 MHz, $CDCl_3$, rt) spectrum of [Au(P^tBu_3)(OAc)].

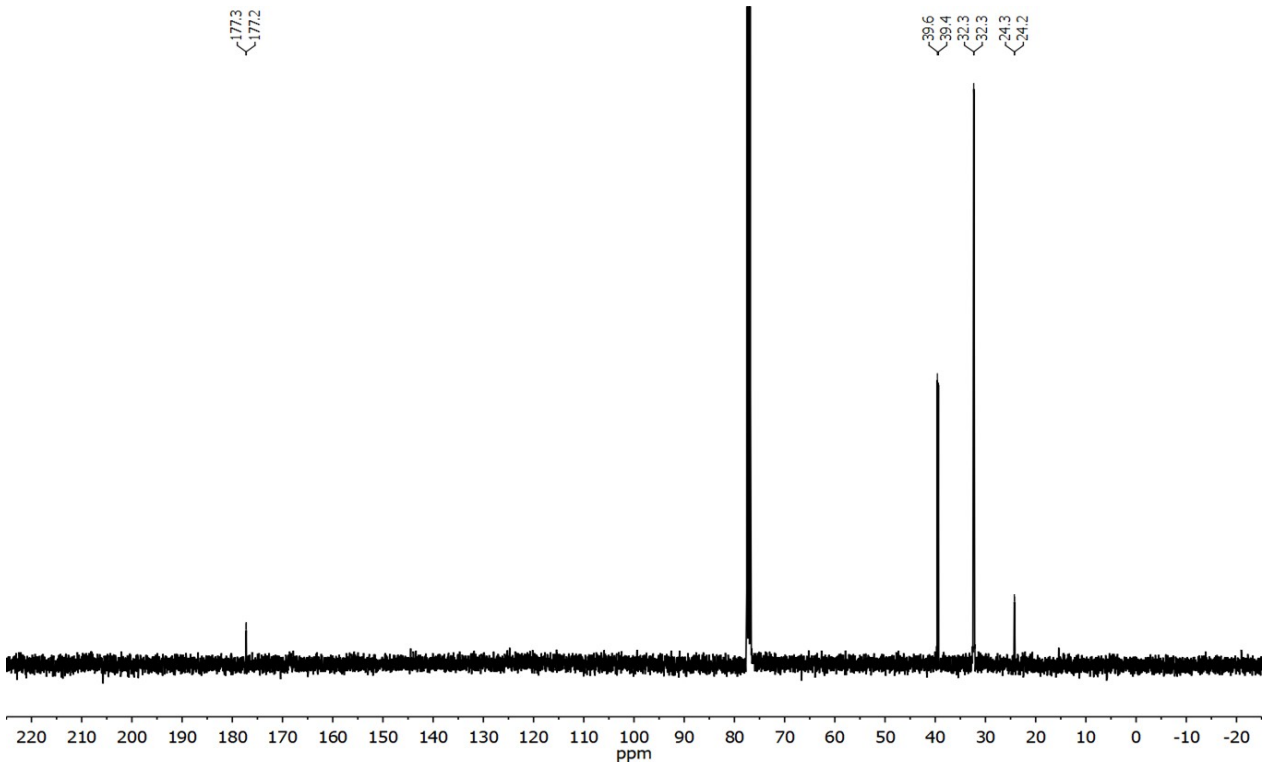

Figure S12. $^{13}C\{^{1}H\}$ NMR (101 MHz, $CDCl_3$, rt) spectrum of [Au(P^tBu_3)(OAc)].

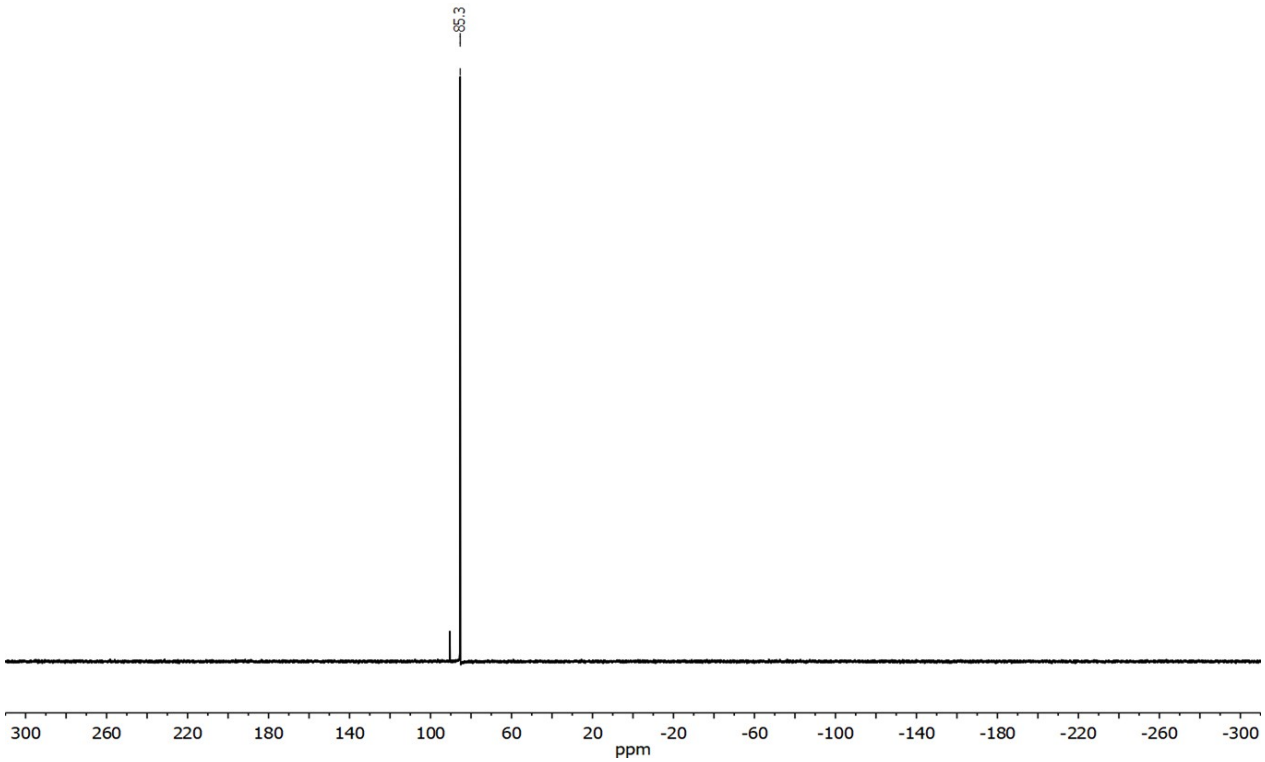

Figure S13. $^{31}P\{^{1}H\}$ NMR (162 MHz, $CDCl_3$, rt) spectrum of [Au(P^tBu_3)(OAc)].

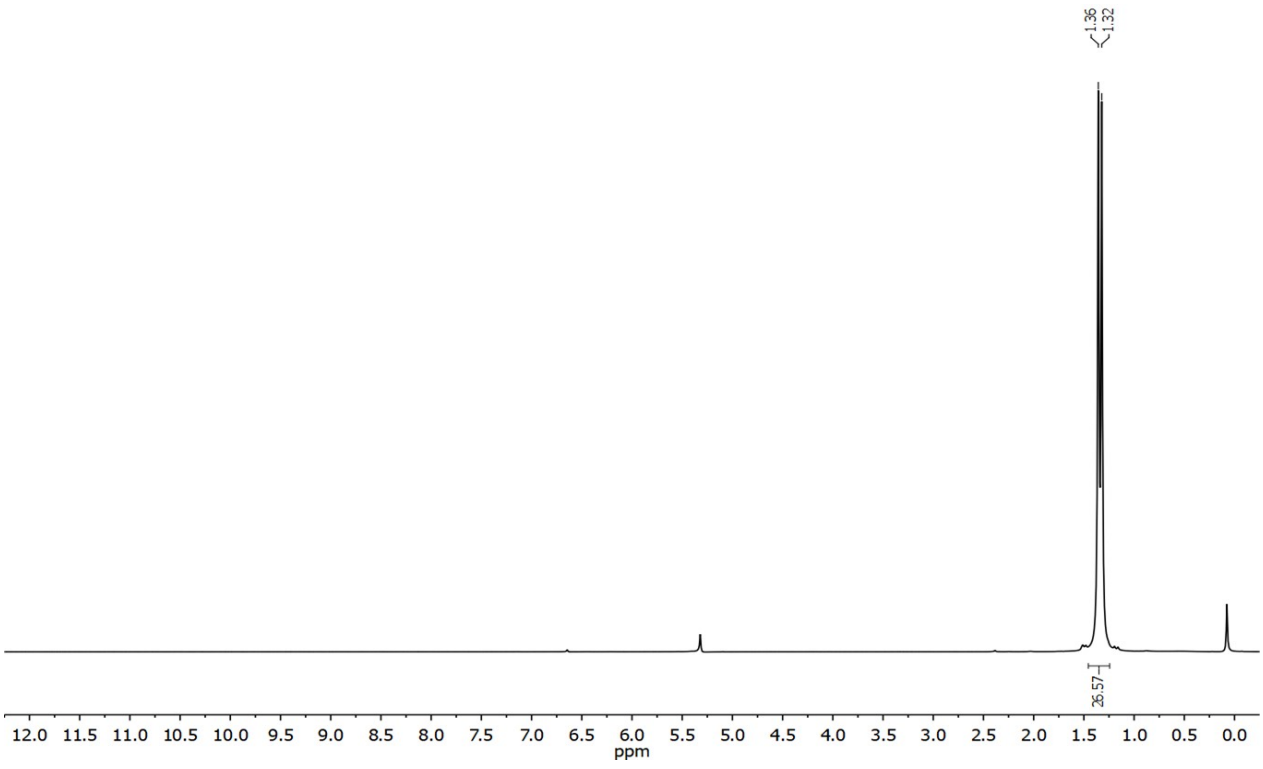

Figure S14. ^{1}H NMR (400 MHz, CD_2Cl_2, rt) spectrum of [Cu($C_5(CF_3)_5$)(P^tBu_3)].

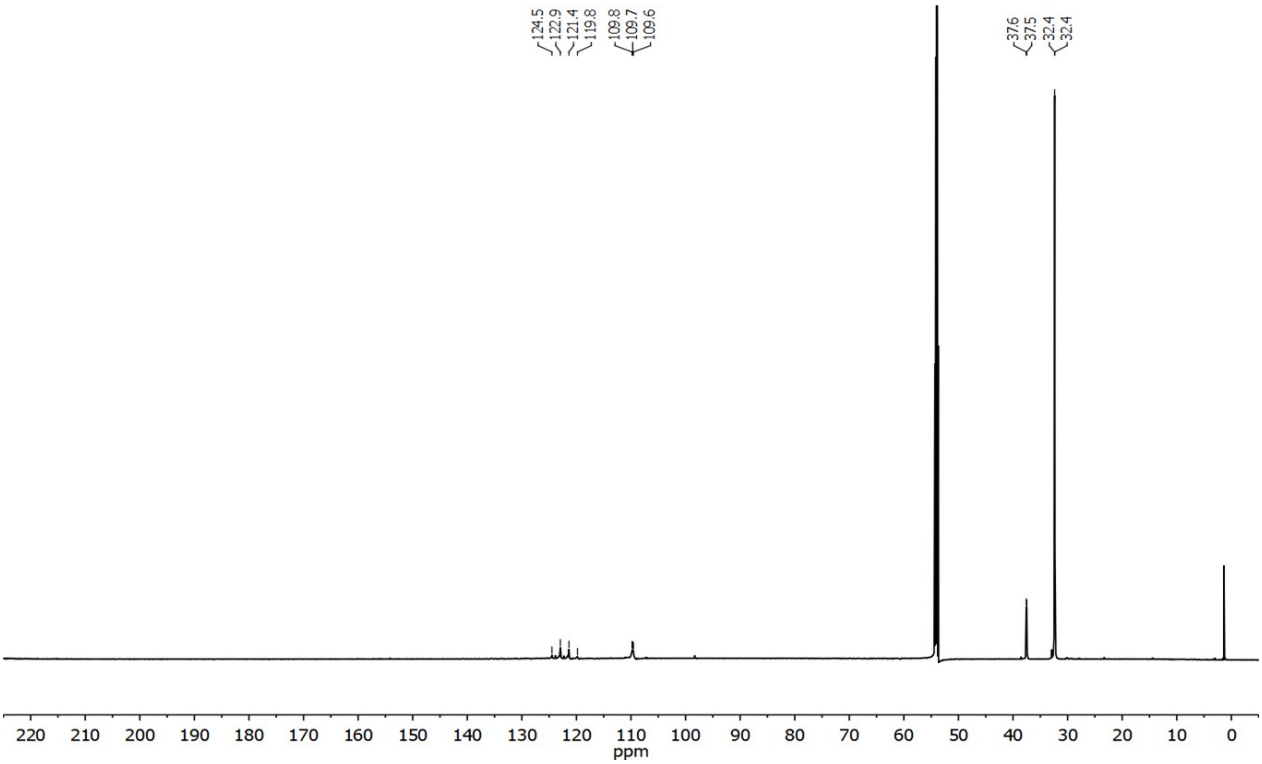

Figure S15. $^{13}C\{^{1}H\}$ NMR (176 MHz, CD_2Cl_2, rt) spectrum of $[Cu(C_5(CF_3)_5)(P^tBu_3)]$.

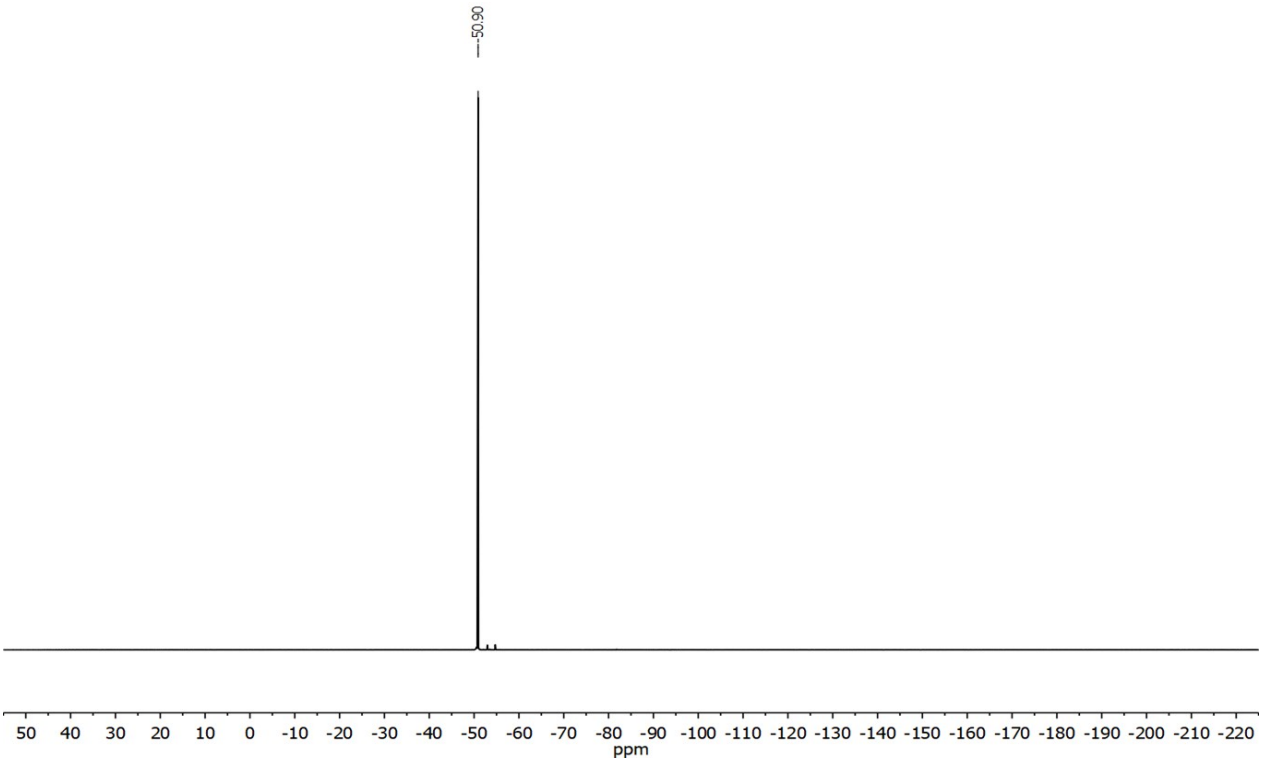

Figure S16. ^{19}F NMR (377 MHz, CD_2Cl_2, rt) spectrum of $[Cu(C_5(CF_3)_5)(P^tBu_3)]$.

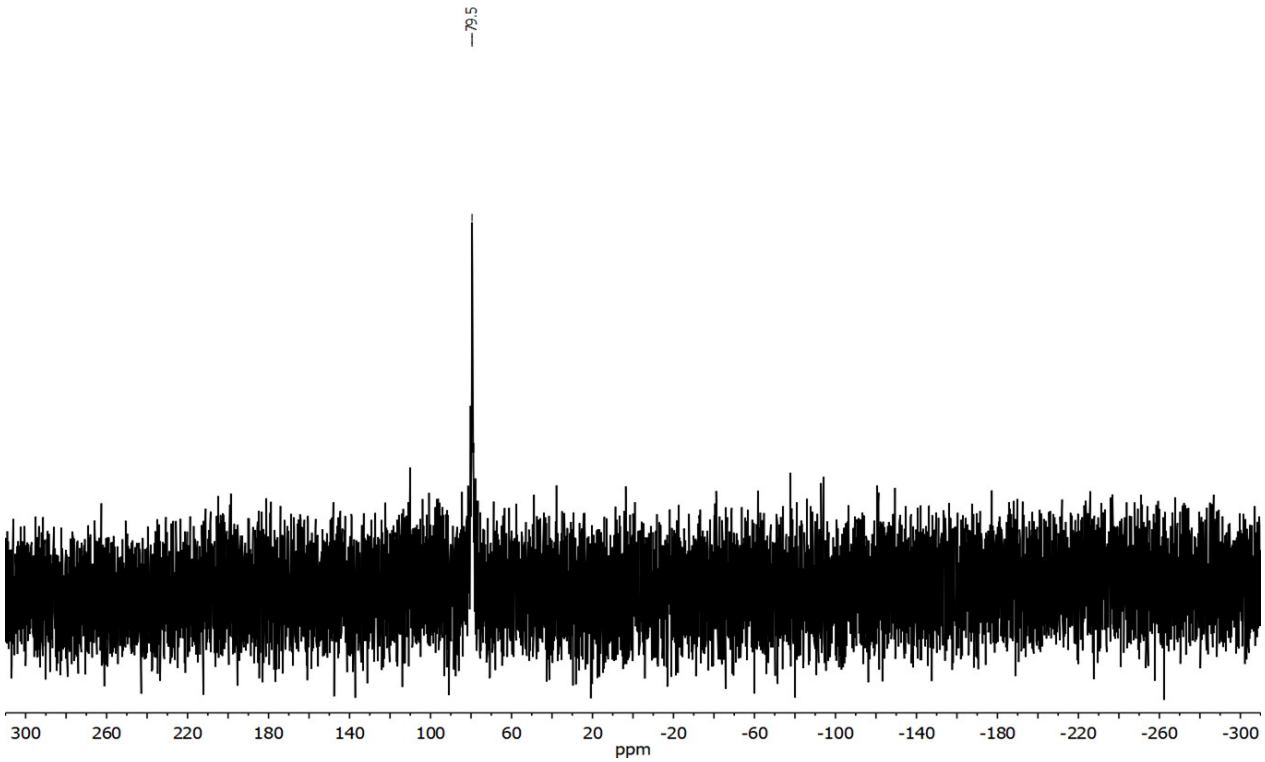

Figure S17. $^{31}P\{^{1}H\}$ NMR (162 MHz, CD_2Cl_2, rt) spectrum of $[Cu(C_5(CF_3)_5)(P^tBu_3)]$.

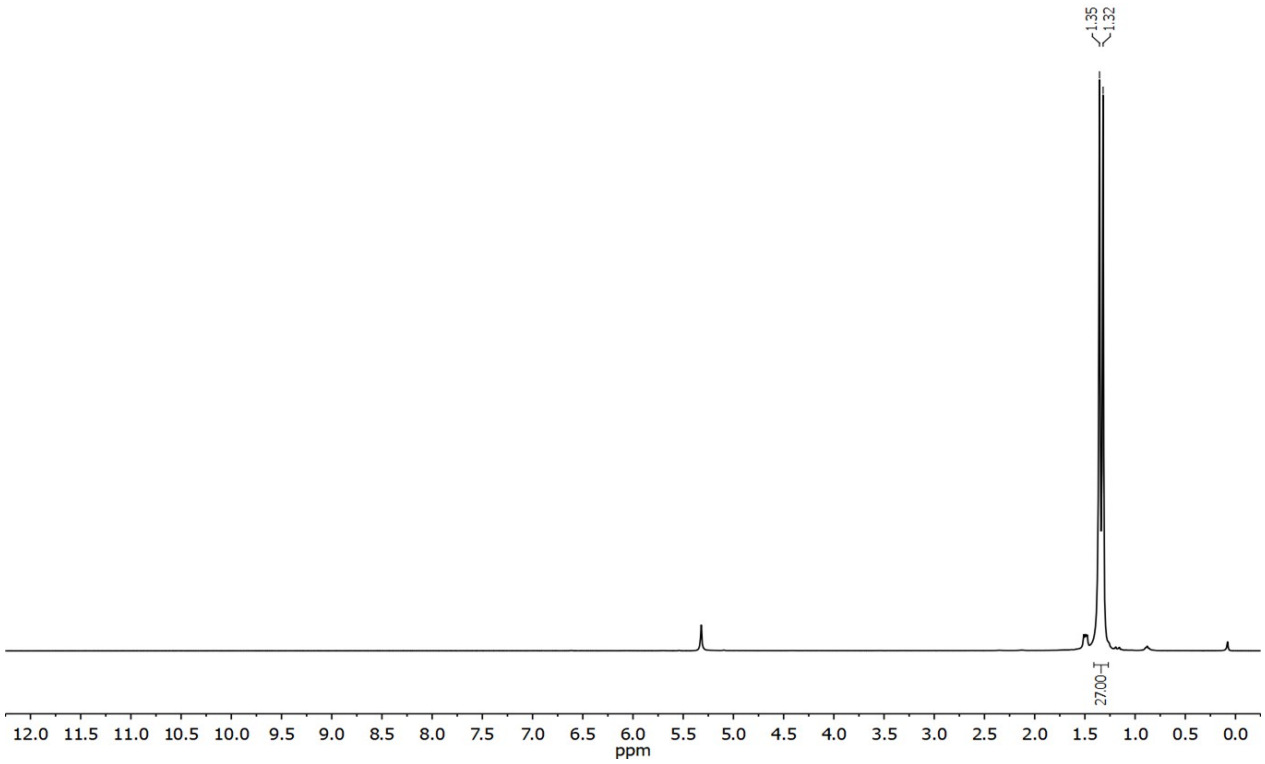

Figure S18. ^{1}H NMR (400 MHz, CD_2Cl_2, rt) spectrum of $[Ag(C_5(CF_3)_5)(P^tBu_3)]$.

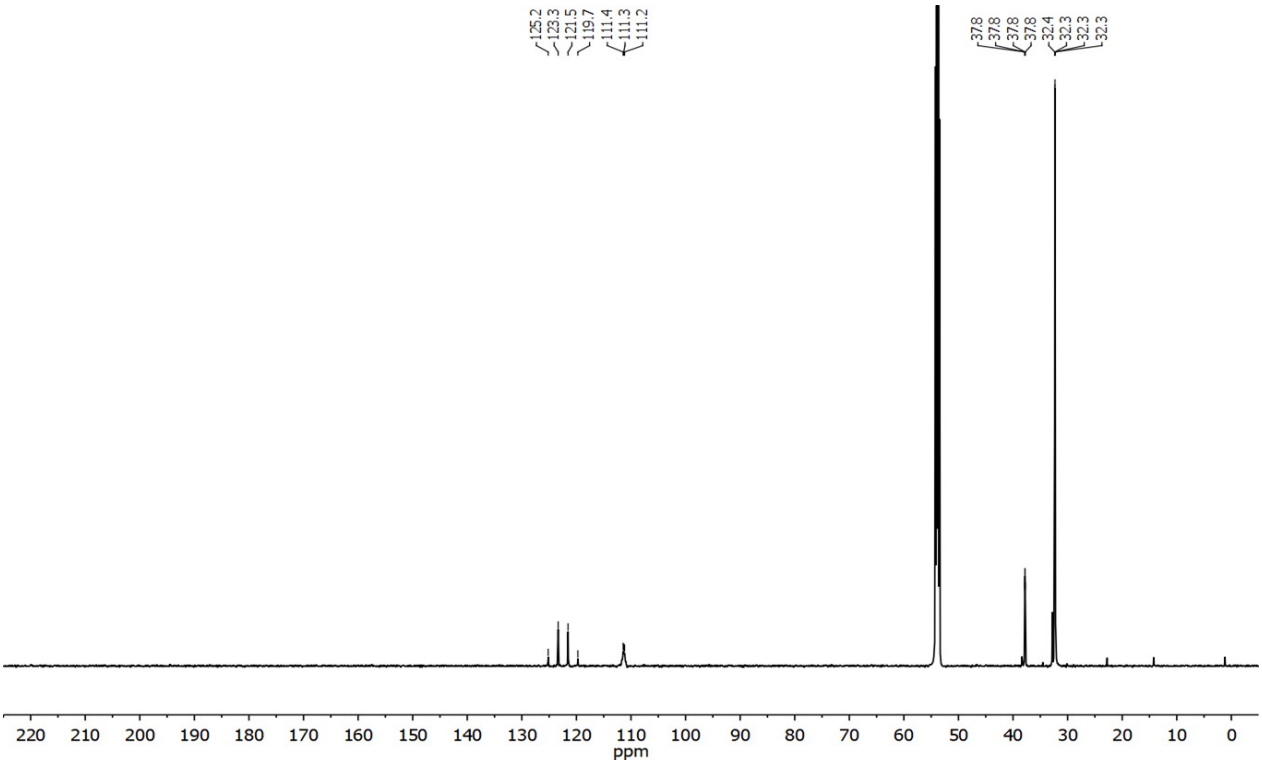

Figure S19. $^{13}C\{^{1}H\}$ NMR (151 MHz, CD_2Cl_2, rt) spectrum of $[Ag(C_5(CF_3)_5)(P^tBu_3)]$.

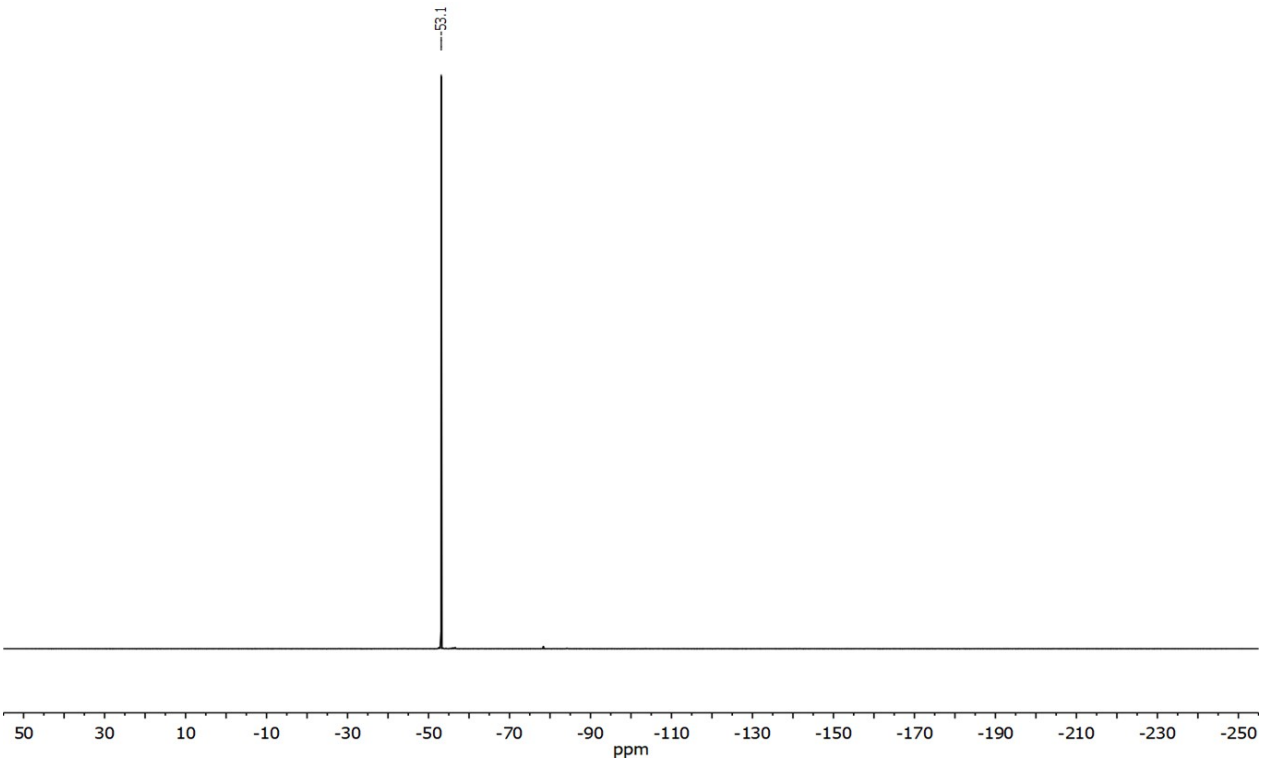

Figure S20. ^{19}F NMR (377 MHz, CD_2Cl_2, rt) spectrum of $[Ag(C_5(CF_3)_5)(P^tBu_3)]$.

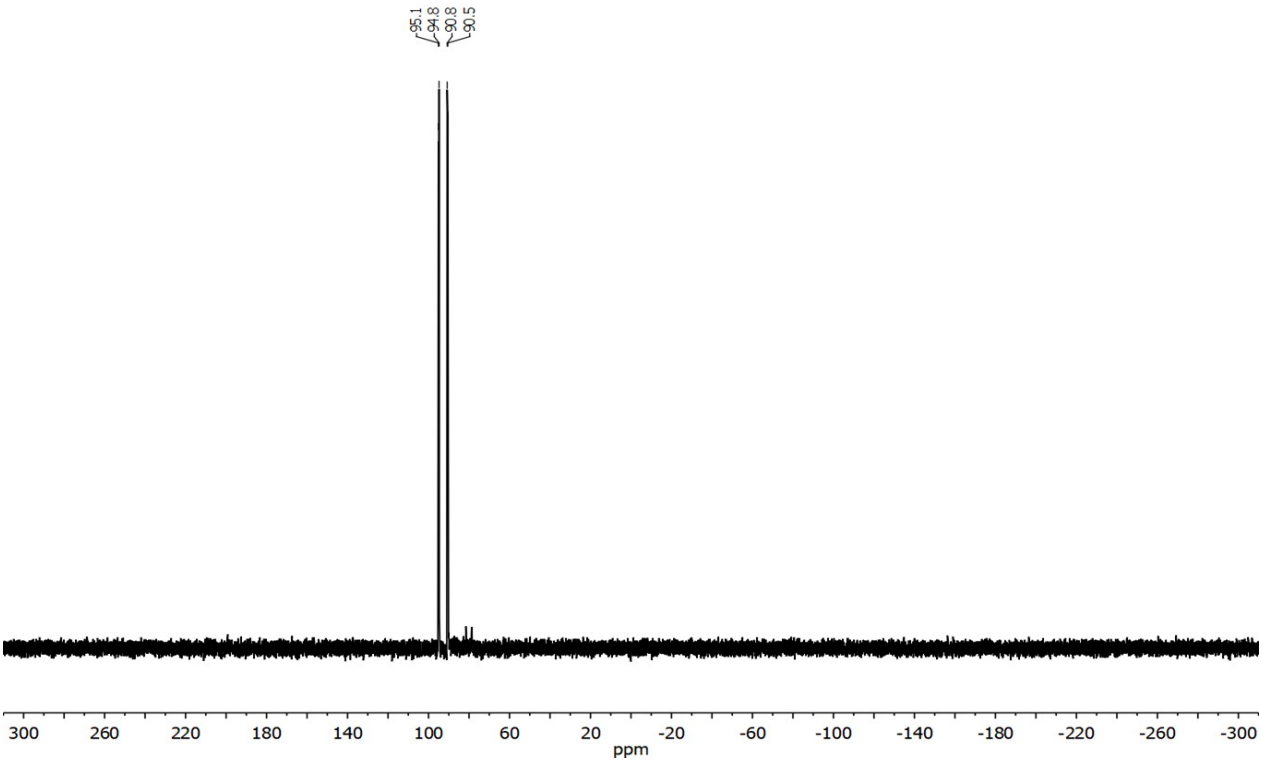

Figure S21. $^{31}P\{^{1}H\}$ NMR (162 MHz, CD_2Cl_2, rt) spectrum of $[Ag(C_5(CF_3)_5)(P^tBu_3)]$.

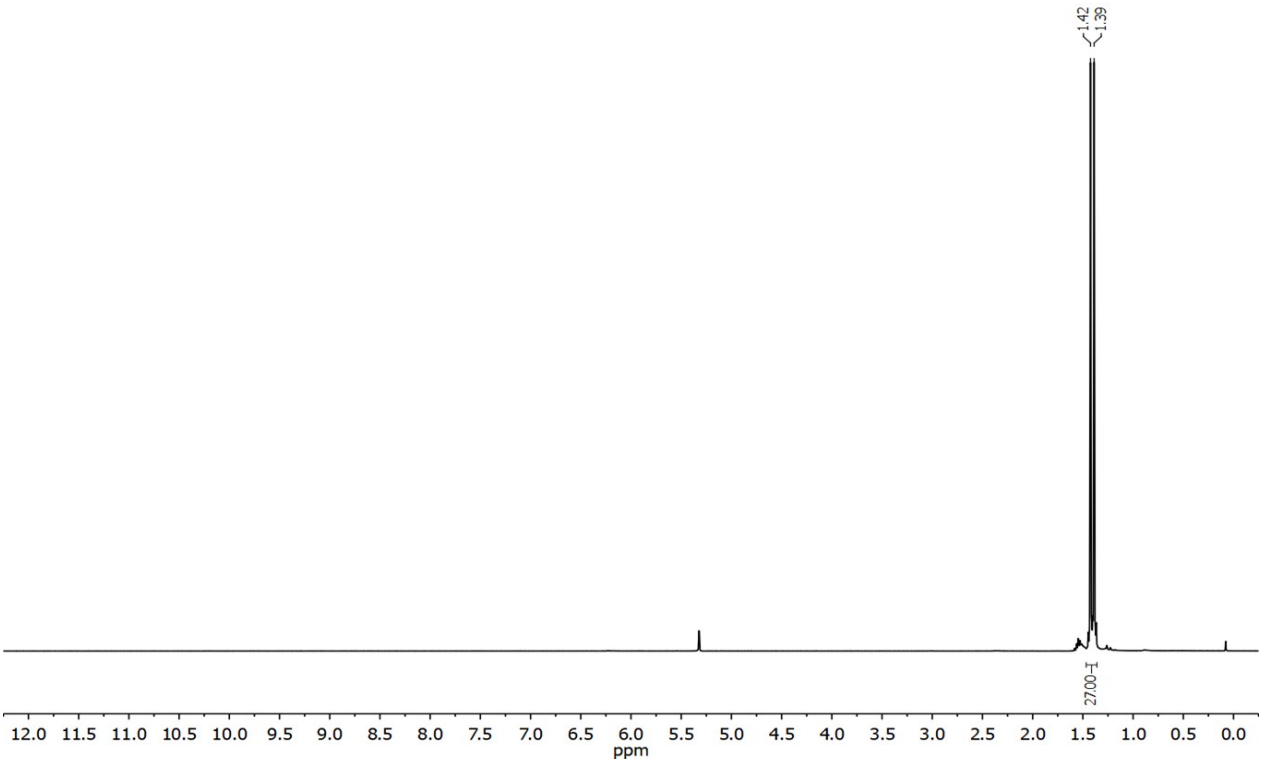

Figure S22. ^{1}H NMR (400 MHz, CD_2Cl_2, rt) spectrum of $[Au(C_5(CF_3)_5)(P^tBu_3)]$.

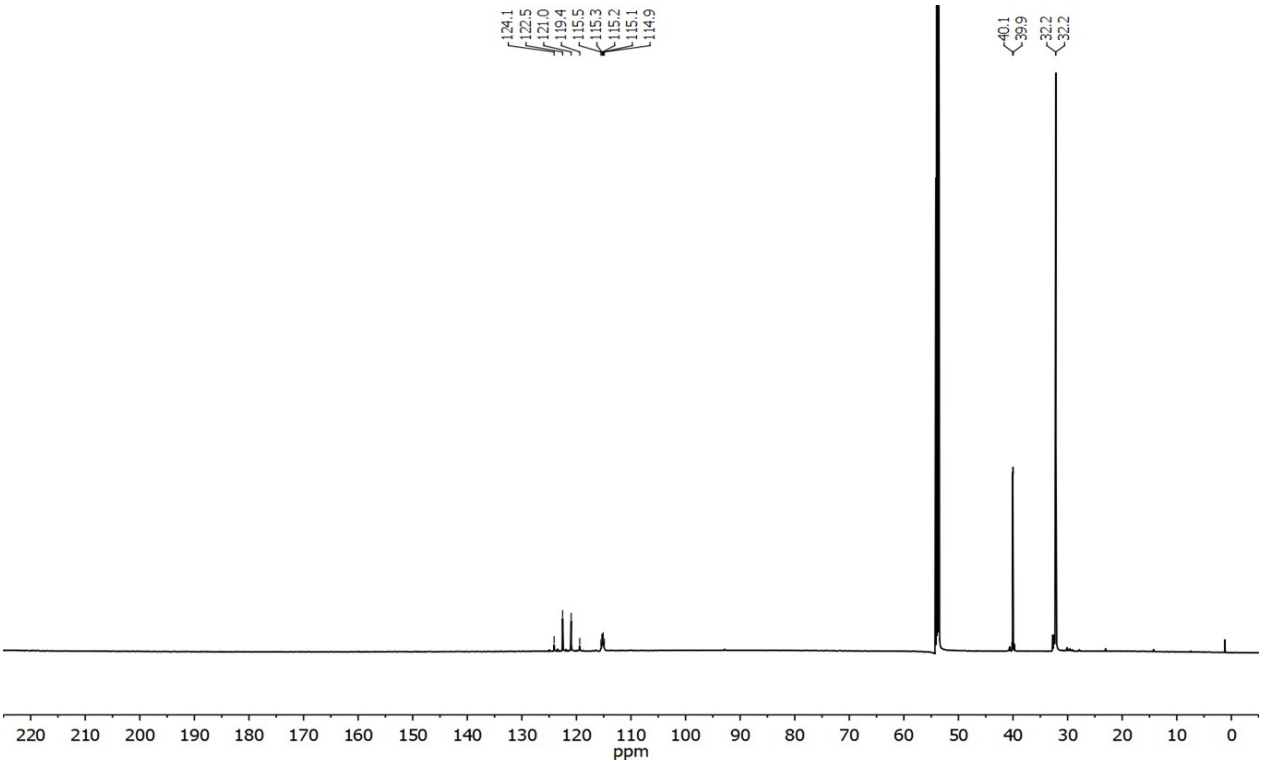

Figure S23. $^{13}C\{^{1}H\}$ NMR (176 MHz, CD_2Cl_2, rt) spectrum of $[Au(C_5(CF_3)_5)(P^tBu_3)]$.

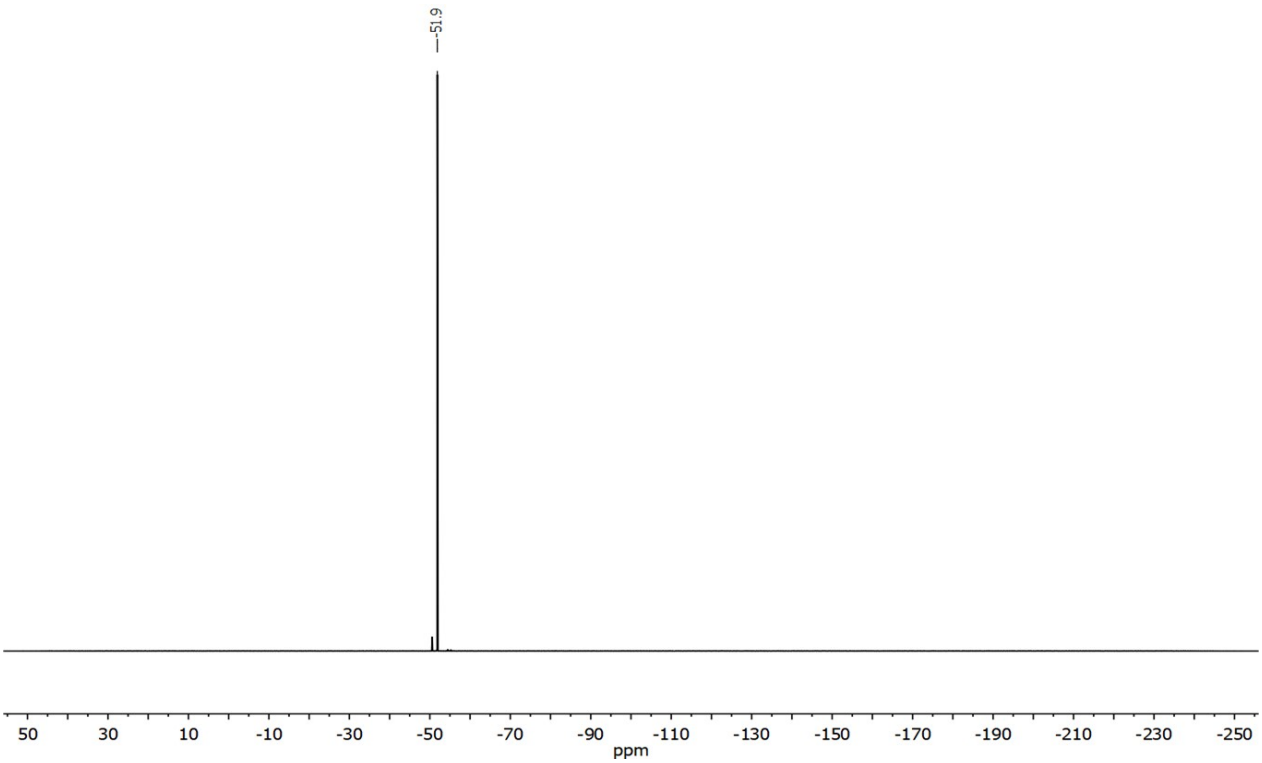

Figure S24. ^{19}F NMR (377 MHz, CD_2Cl_2, rt) spectrum of $[Au(C_5(CF_3)_5)(P^tBu_3)]$.

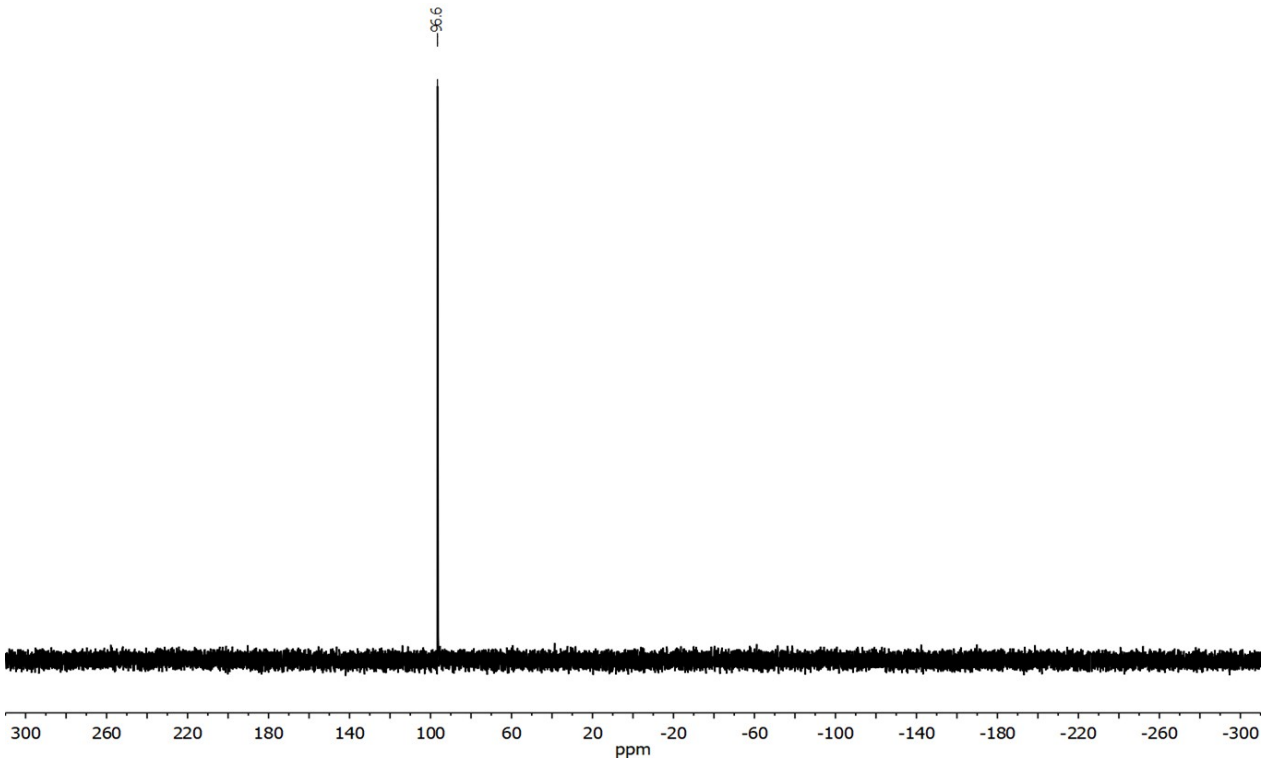

Figure S25. $^{31}P\{^{1}H\}$ NMR (162 MHz, CD_2Cl_2, rt) spectrum of $[Au(C_5(CF_3)_5)(P^tBu_3)]$.

IR Spectra

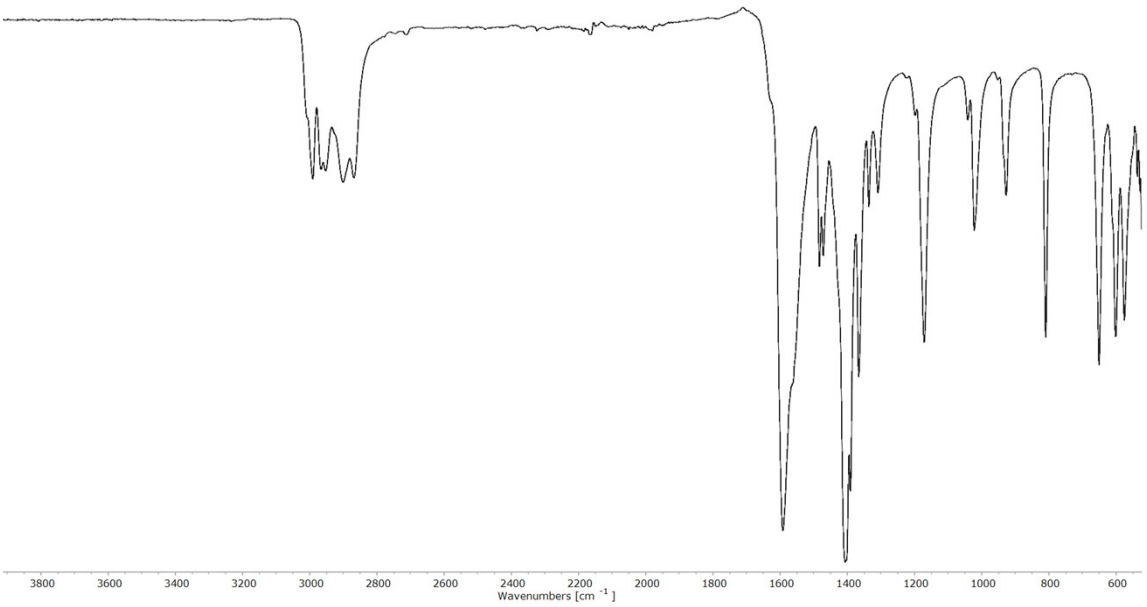

Figure S26. IR (ATR, rt) spectrum of [Cu(P^{t}Bu$_3$)(OAc)].

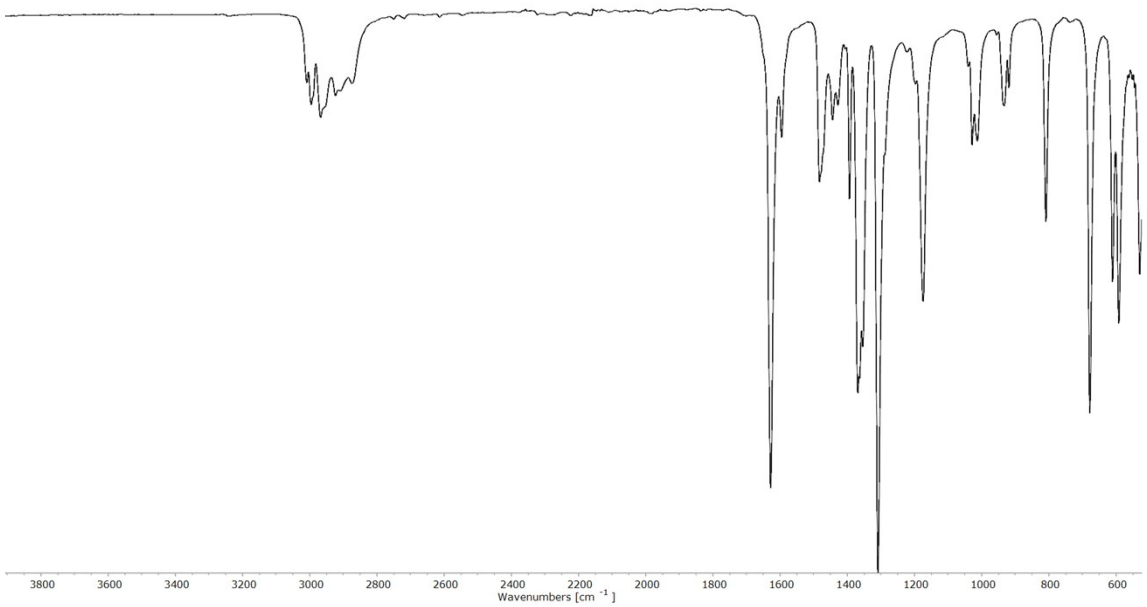

Figure S27. IR (ATR, rt) spectrum of [Au(P^{t}Bu$_3$)(OAc)].

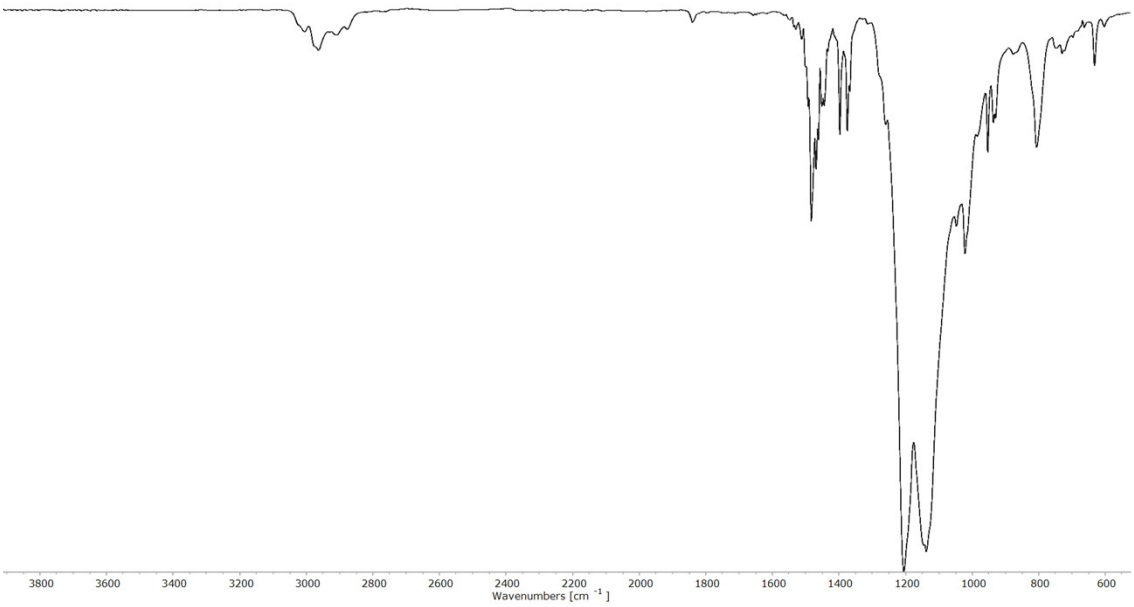

Figure S28. IR (ATR, rt) spectrum of $[Cu(C_5(CF_3)_5)(P^tBu_3)]$.

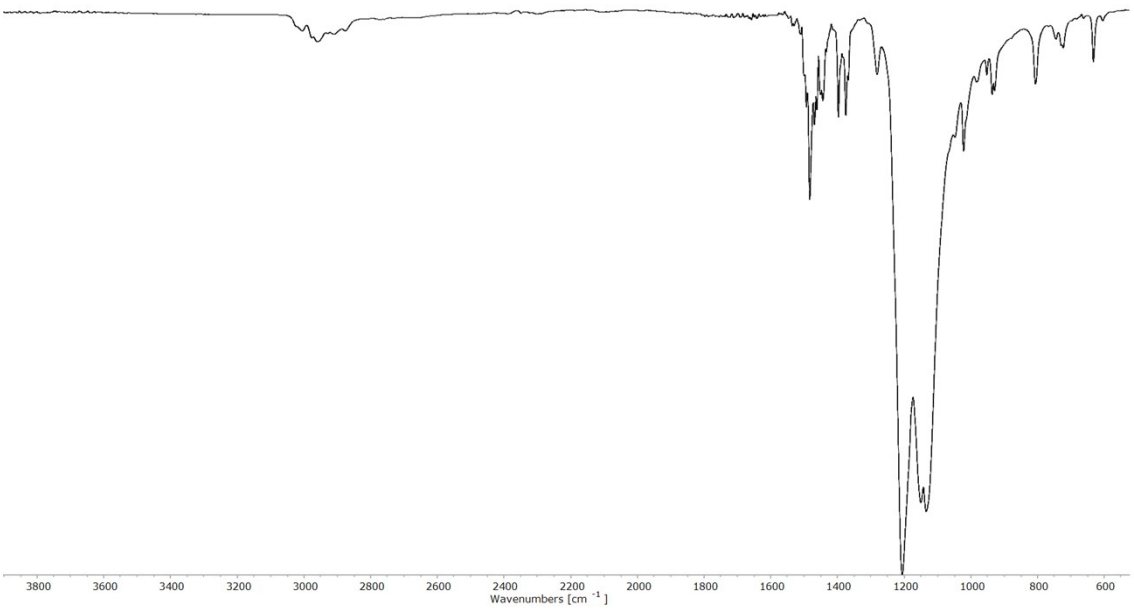

Figure S29. IR (ATR, rt) spectrum of $[Ag(C_5(CF_3)_5)(P^tBu_3)]$.

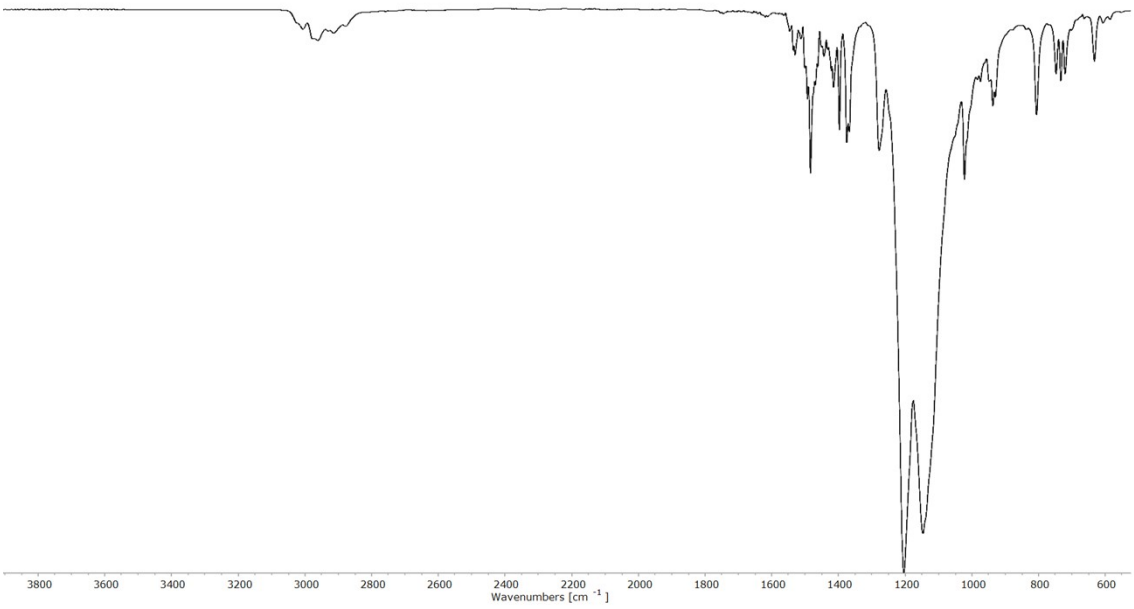

Figure S30. IR (ATR, rt) spectrum of [Au($C_5(CF_3)_5$)(P^tBu_3)].

Crystallographic Data

Table S1. Crystallographic data of [Cu($C_5(CF_3)_5$)(P^tBu_3)].

Identification code	2309684
Empirical formula	$C_{22}H_{27}CuF_{15}P$
Formula weight	670.94
Temperature/K	105.00
Crystal system	monoclinic
Space group	$P2_1/n$
a/Å	9.2818(3)
b/Å	14.7927(5)
c/Å	19.3153(7)
α/°	90
β/°	95.8860(10)
γ/°	90
Volume/Å^3	2638.06(16)
Z	4
ρ_{calc}g/cm^3	1.689
μ/mm^{-1}	1.006
F(000)	1352.0
Crystal size/mm^3	0.1 × 0.1 × 0.1
Radiation	MoKα (λ = 0.71073)
2Θ range for data collection/°	4.24 to 53.496
Index ranges	-11 ≤ h ≤ 11, -17 ≤ k ≤ 18, -24 ≤ l ≤ 24
Reflections collected	43658
Independent reflections	5606 [R_{int} = 0.0331, R_{sigma} = 0.0197]
Data/restraints/parameters	5606/0/499
Goodness-of-fit on F^2	1.060
Final R indexes [I>=2σ (I)]	R_1 = 0.0658, wR_2 = 0.1896
Final R indexes [all data]	R_1 = 0.0764, wR_2 = 0.2008
Largest diff. peak/hole / e Å^{-3}	1.51/-0.56

Table S2. Crystallographic data of $[Ag(C_5(CF_3)_5)(P^tBu_3)]$.

Identification code	2309685
Empirical formula	$C_{22}H_{27}AgF_{15}P$
Formula weight	715.27
Temperature/K	105.00
Crystal system	triclinic
Space group	*P*-1
a/Å	9.4791(8)
b/Å	10.7301(9)
c/Å	14.7059(13)
α/°	90.169(3)
β/°	90.230(3)
γ/°	116.097(3)
Volume/Å^3	1343.2(2)
Z	2
ρ_{calc}g/cm^3	1.768
μ/mm^{-1}	0.925
F(000)	712.0
Crystal size/mm^3	0.1 × 0.1 × 0.1
Radiation	MoKα (λ = 0.71073)
2Θ range for data collection/°	4.786 to 56.874
Index ranges	-12 ≤ h ≤ 12, -14 ≤ k ≤ 13, -19 ≤ l ≤ 19
Reflections collected	25494
Independent reflections	6637 [R_{int} = 0.0498, R_{sigma} = 0.0461]
Data/restraints/parameters	6637/0/362
Goodness-of-fit on F^2	1.082
Final R indexes [I>=2σ (I)]	R_1 = 0.0403, wR_2 = 0.1148
Final R indexes [all data]	R_1 = 0.0424, wR_2 = 0.1169
Largest diff. peak/hole / e Å^{-3}	0.97/-1.02

Table S3. Crystallographic data of $[Au(C_5(CF_3)_5)(P^tBu_3)]$.

Identification code	2309686
Empirical formula	$C_{22}H_{27}AuF_{15}P$
Formula weight	804.37
Temperature/K	105.00
Crystal system	triclinic
Space group	*P*-1
a/Å	10.7338(3)
b/Å	17.1617(6)
c/Å	17.3230(6)
α/°	112.2220(10)
β/°	102.5950(10)
γ/°	104.5520(10)
Volume/Å^3	2679.07(15)
Z	4
ρ_{calc}g/cm^3	1.994
μ/mm^{-1}	11.981
F(000)	1552.0
Crystal size/mm^3	0.1 × 0.1 × 0.1
Radiation	CuKα (λ = 1.54178)
2Θ range for data collection/°	5.882 to 144.752
Index ranges	-13 ≤ h ≤ 12, -21 ≤ k ≤ 19, 0 ≤ l ≤ 21
Reflections collected	10209
Independent reflections	10209 [R_{int} = ?, R_{sigma} = 0.0341]
Data/restraints/parameters	10209/0/722
Goodness-of-fit on F^2	1.126
Final R indexes [I>=2σ (I)]	R_1 = 0.0332, wR_2 = 0.1030
Final R indexes [all data]	R_1 = 0.0362, wR_2 = 0.1068
Largest diff. peak/hole / e Å^{-3}	1.15/-1.72

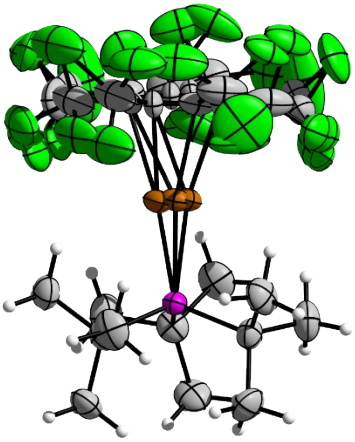

Figure S31. Molecular structure in the solid state of [Cu($C_5(CF_3)_5$)(P^tBu_3)] with crystallographic disordering. Ellipsoids are depicted with 50 % probability level. Color code: white-hydrogen, grey-carbon, green-fluorine, purple-phosphorous, brown-copper.[29]

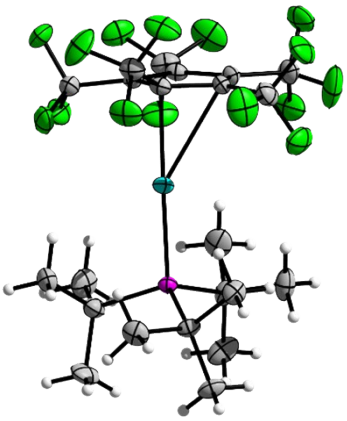

Figure S32. Molecular structure in the solid state of [Ag($C_5(CF_3)_5$)(P^tBu_3)]. Ellipsoids are depicted with 50 % probability level. Color code: white-hydrogen, grey-carbon, green-fluorine, purple-phosphorous, blue-silver.

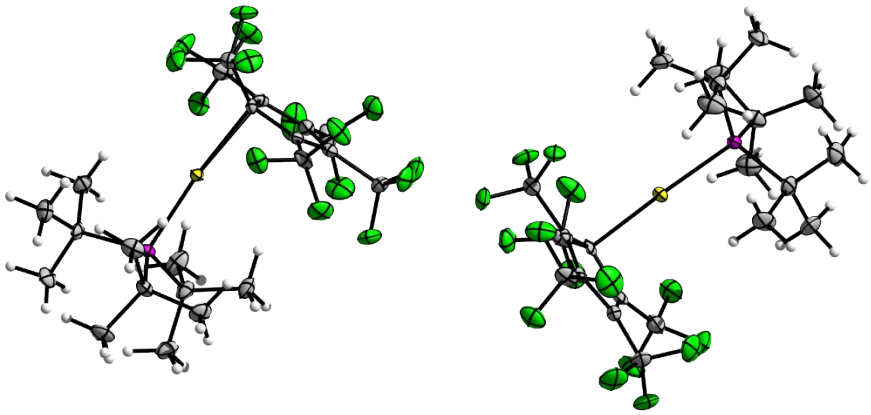

Figure S33. Molecular structure in the solid state of [Au($C_5(CF_3)_5$)(P^tBu_3)]. Ellipsoids are depicted with 50 % probability level. Color code: white-hydrogen, grey-carbon, green-fluorine, purple-phosphorous, yellow-gold.[30]

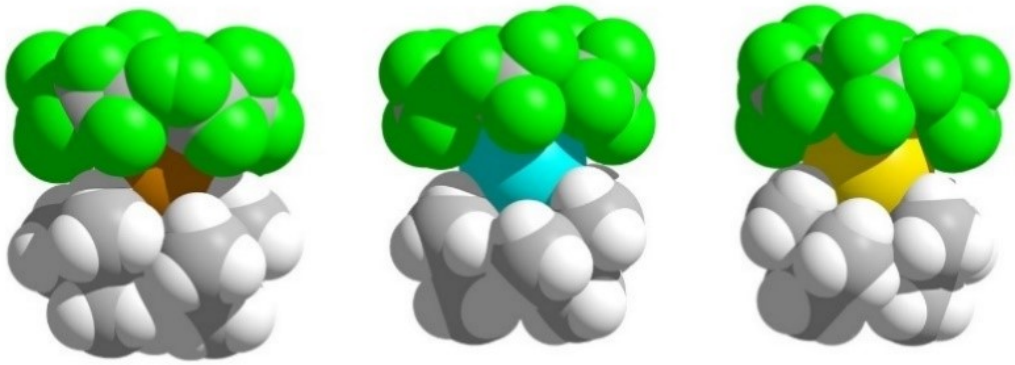

Figure S34. Space filling representation of [M($C_5(CF_3)_5$)(P^tBu_3)] (M = Cu (left), Ag (middle), Au (right)).

DFT Calculations

Table S4. Selected optimized bond lengths [Å] of [M($C_5(CF_3)_5$)(P^tBu_3)] (M = Cu, Ag, Au) (see table 1 for abbreviations). ZORA-r^{2}SCAN-3c results.

Atom distance	[Cu($C_5(CF_3)_5$)(P^tBu_3)]	[Ag($C_5(CF_3)_5$)(P^tBu_3)]	[Au($C_5(CF_3)_5$)(P^tBu_3)]
M-C_1	2.057	2.272	2.214
M-C_2	2.502	2.698	2.738
M-C_3	2.917	3.306	3.378
M-C_4	2.741	3.320	3.377
M-C_5	2.201	2.719	2.731
C_1-C_2	1.435	1.441	1.457
C_2-C_3	1.412	1.401	1.388
C_3-C_4	1.416	1.425	1.435
C_4-C_5	1.423	1.403	1.389
C_5-C_1	1.443	1.445	1.461

Table S5. Selected optimized bond lengths [Å] of [M($C_5(CF_3)_5$)(P^tBu_3)] (M = Cu, Ag, Au) (see table 1 for abbreviations). Nonrelativistic r^{2}SCAN-3c results.

Atom distance	[Cu($C_5(CF_3)_5$)(P^tBu_3)]	[Ag($C_5(CF_3)_5$)(P^tBu_3)]	[Au($C_5(CF_3)_5$)(P^tBu_3)]
M-C_1	2.081	2.370	2.573
M-C_2	2.499	2.626	2.588
M-C_3	2.900	3.138	2.668
M-C_4	2.731	3.226	2.634
M-C_5	2.219	2.754	2.605
C_1-C_2	1.434	1.434	1.429
C_2-C_3	1.414	1.414	1.425
C_3-C_4	1.417	1.419	1.422
C_4-C_5	1.423	1.411	1.422
C_5-C_1	1.441	1.432	1.427

Table S6. Selected optimized bond lengths [Å] of [M($C_5(CF_3)_5$)(PMe_3)] (M = Cu, Ag, Au) (see table 1 for abbreviations). ZORA-r^{2}SCAN-3c results.

Atom distance	[Cu($C_5(CF_3)_5$)(PMe_3)]	[Ag($C_5(CF_3)_5$)(PMe_3)]	[Au($C_5(CF_3)_5$)(PMe_3)]
M-C_1	2.031	2.292	2.189
M-C_2	2.329	2.624	2.790
M-C_3	2.763	3.170	3.473
M-C_4	2.717	3.216	3.446
M-C_5	2.258	2.696	2.746
C_1-C_2	1.444	1.441	1.463
C_2-C_3	1.415	1.404	1.383
C_3-C_4	1.420	1.424	1.438
C_4-C_5	1.416	1.404	1.384
C_5-C_1	1.442	1.443	1.466

Table S7. Selected optimized bond lengths [Å] of [M($C_5(CF_3)_5$)(PMe_3)] (M = Cu, Ag, Au) (see table 1 for abbreviations). Nonrelativistic r^{2}SCAN-3c results.

Atom distance	[Cu($C_5(CF_3)_5$)(PMe_3)]	[Ag($C_5(CF_3)_5$)(PMe_3)]	[Au($C_5(CF_3)_5$)(PMe_3)]
M-C_1	2.057	2.368	2.355
M-C_2	2.339	2.688	2.621
M-C_3	2.756	3.236	3.108
M-C_4	2.710	3.285	3.152
M-C_5	2.270	2.759	2.673
C_1-C_2	1.442	1.434	1.433
C_2-C_3	1.426	1.409	1.414
C_3-C_4	1.420	1.420	1.420
C_4-C_5	1.416	1.409	1.412
C_5-C_1	1.440	1.435	1.435

Table S8. Natural atomic charges in [M($C_5(CF_3)_5$)(PMe_3)]] obtained from natural population analysis at the ZORA and nonrelativistic r^{2}SCAN-3c level.

M	q(M)	q(PMe_3)	q($C_5(CF_3)_5$)	q(P)	q(C_1)	q(C_2)	q(C_3)	q(C_4)	q(C_5)
Cu	0.630	0.307	–0.937	0.729	–0.341	–0.177	–0.168	–0.173	–0.186
Ag	0.596	0.311	–0.907	0.731	–0.398	–0.124	–0.144	–0.149	–0.125
Au	0.320	0.446	–0.766	0.876	–0.388	–0.227	–0.178	–0.173	–0.211
Cu[a]	0.648	0.295	–0.943	0.719	–0.320	–0.188	–0.172	–0.178	–0.198
Ag[a]	0.687	0.254	–0.941	0.618	–0.298	–0.216	–0.177	–0.173	–0.204
Au[a]	0.654	0.280	–0.934	0.717	–0.330	–0.230	–0.180	–0.173	–0.214

[a] Calculations were performed without inclusion of scalar relativistic effects.

Table S9. Contributions to the binding energy [kJ/mol] between a [Ag-PMe_3]$^+$ and a [$C_5(CX_3)_5$]$^-$ (X = H, F) fragment at the scalar relativistic ZORA-r^{2}SCAN-3c level.

$[C_5(CX_3)_5]^-$	ΔE_{Pauli}	$\Delta E_{Elstat.}$	$\Delta E_{Orb.Int.}$	ΔE_{Total}
X = H (η^5)	310.4	–684.5	–255.5	–636.5
X = H (η^3/η^1)	290.3	–673.7	–227.1	–619.7
X = F (η^5)	284.7	–498.9	–190.7	–414.8
X = F (η^3/η^1)	237.8	–493.6	–168.3	–436.1

References

[1] H. E. Gottlieb, V. Kotlyar, A. Nudelman, *J. Org. Chem.*, 1997, **62**, 7512–7515.

[2] G. R. Fulmer, A. J. M. Miller, N. H. Sherden, H. E. Gottlieb, B. M. Stoltz, J. E. Bercaw, K. I. Goldberg, *Organometallics*, 2010, **29**, 2176–2179.

[3] R. K. Harris, E. D. Becker, S. M. Cabral de Menezes, R. Goodfellow, P. Granger, *Pure Appl. Chem.*, 2001, **73**, 1795–1818.

[4] M. R. Willcott, *J. Am. Chem. Soc.*, 2009, **131**, 13180.

[5] O. V. Dolomanov, L. J. Bourhis, R. J. Gildea, J. A. K. Howard, H. Puschmann, *J. Appl. Cryst.*, 2009, **42**, 339–341.

[6] G. M. Sheldrick, *Acta Cryst.*, 2015, **A71**, 3–8.

[7] G. M. Sheldrick, *SHELXL Version 2014/7, Program for Crystal Structure Solution and Refinement*; Göttingen, Germany, 2014.

[8] G. M. Sheldrick, *Acta Cryst.*, 2008, **A64**, 112–122.

[9] K. Brandenburg, Diamond: Crystal and Molecular Structure Visualization http://www.crystalimpact.com/diamond.

[10] Persistence of Vision Pty. Ltd. Persistence of Vision Raytracer. Ltd., Persistence of Vision Pty. 2004.

[11] T. Gasevic, J. B. Stückrath, S. Grimme, M. Bursch, *J. Phys. Chem.*, 2022, **126**, 3826–3838.

[12] G. te Velde, F. M. Bickelhaupt, E. J. Baerends, C. Fonseca Guerra, S. J. A. van Gisbergen, J. G. Snijder, T. Ziegler, *J. Comput. Chem.*, 2001, **22**, 931–967.

[13] AMS 2022.1, SCM, Theoretical Chemistry, Vrije Universiteit, Amsterdam, The Netherlands, http://www.scm.com (accessed 2023-09-04).

[14] E. van Lenthe, A. Ehlers, E. Baerends, *J. Chem. Phys.*, 1999, **110**, 8943–8953.

[15] A. E. Reed, R. B. Weinstock, F. Weinhold, *J. Chem. Phys.*, 1985, **83**, 735–746.

[16] T. Ziegler, A. Rauk, *Theor. Chim. Acta*, 1977, **46**, 1–10.

[17] Q. Ma, H. Werner, *J. Chem. Theory Comput.*, 2018, **14**, 198–215.

[18] Q. Ma, H. Werner, *J. Chem Theory Comput.*, 2020, **16**, 3135–3151.

[19] H. Werner, P. J. Knowles, F. R. Manby, J. A. Black, K. Doll, A. Heßelmann, D. Kats, A. Köhn, T. Korona, D. A. Kreplin, Q. Ma, T. F. Miller, A. Mitrushchenkov, K. A. Peterson, I. Polyak, G. Rauhut, M. Sibaev, *J. Chem. Phys.*, 2020, **152**, 144107.

[20] MOLPRO V2022.2, a Package of ab initio Programs, H. Werner, P. J. Knowles, G. Knizia, F. R. Manby, M. Schütz, P. Celani, W. Györffy, D. Kats, T. Korona, R. Lindh, A. Mitrushenkov, G. Rauhut, K. R. Shamasundar, T. B. Adler, R. D. Amos, S. J. Bennie, A. Bernhardsson, A. Berning, D. L. Cooper, M. J. O. Deegan, A. J. Dobbyn, F. Eckert, E. Goll, C. Hampel, A. Hesselmann, G. Hetzer, T. Hrenar, G. Jansen, C. Köppl, S. J. R. Lee, Y. Liu, A. W. Lloyd, Q. Ma, R. A. Mata, A. J. May, S. J. McNicholas, W. Meyer, T. F. Miller III, M. E. Mura, A. Nicklass, D. P. O'Neill, P. Palmieri, D. Peng, K. Pflüger, R. Pitzer, M. Reiher, T. Shiozaki, H. Stoll, A. J. Stone, R. Tarroni, T. Thorsteinsson, M. Wang, and M. Welborn, see https://www.molpro.net (accessed 2023-11-10).

[21] K. A. Peterson, T. B. Adler, H. Werner, *J. Chem. Phys.*, 2008, **128**, 084102.

[22] According to NMR spectroscopy, the product mixture consists of 85 mol% $[NEt_4][C_5(CF_3)_5]$ and 15 mol% $[NEt_4][C_5(CF_3)_4H]$, which are inseperable.

[23] E. P. Janulis, A. J. Arduengo, *J. Am. Chem. Soc.*, 1983, **105**, 3563–3567.

[24] R. D. Chambers, W. K. Gray, J. F. S. Vaughan, S. R. Korn, M. Médebielle, A. S. Batsanov, C. W. Lehmann, J. A. K. Howard, *Perkin Trans.*, 1997, 135–146.

[25] R. Sievers, M. Sellin, S. M. Rupf, M. Malischewski, *Angew. Chem. Int. Ed.*, 2022, *e202211147*.

[26] The Carbonyl-carbon is invisible in $^{13}C\{^1H\}$ NMR spectroscopy due to pronounced C-Cu-coupling patterns, even with prolonged measuring times.

[27] R. G. Goel, P. Pilon, *Inorg. Chem.*, 1978, **17**, 2876–2879.

[28] The stated yield refers to the applied amount of substance of $[M(P^tBu_3)(OAc)]$ (M = Cu, Ag, Au).

[29] Distances and angles (see table 1) were measured from the structure with the highest probability.

[30] Distances and angles (see table 1) were averaged from the two asymmetric units.